The International Association for the Properties of Water and Steam

Lucerne, Switzerland
August 2007

Revised Release on the IAPWS Industrial Formulation 1997 for the Thermodynamic Properties of Water and Steam

(The revision only relates to the extension of region 5 to 50 MPa)

President:
J. R. Cooper
School of Engineering and Materials Science
Queen Mary, University of London
Mile End Road
London E1 4NS, England

Executive Secretary:
Dr. R. B. Dooley
Structural Integrity Associates, Inc.
2616 Chelsea Drive
Charlotte, NC 28209, USA
email: bdooley@structint.com

This revised release replaces the corresponding release of 1997 and contains 49 pages, including this cover page.

This release has been authorized by the International Association for the Properties of Water and Steam (IAPWS) at its meeting in Lucerne, Switzerland, 26-31 August, 2007, for issue by its Secretariat. The members of IAPWS are: Argentina and Brazil, Britain and Ireland, Canada, the Czech Republic, Denmark, France, Germany, Greece, Italy, Japan, Russia, and the United States of America, and associate member Switzerland.

The formulation provided in this release is recommended for industrial use, and is called "IAPWS Industrial Formulation 1997 for the Thermodynamic Properties of Water and Steam" abbreviated to "IAPWS Industrial Formulation 1997" (IAPWS-IF97). The IAPWS-IF97 replaces the previous Industrial formulation "The 1967 IFC Formulation for Industrial Use" (IFC-67) [1]. Further details about the formulation can be found in the article by W. Wagner et al. [2] and for the extended region 5 in [2a]. Additional supplementary backward equations have been adopted by IAPWS and are listed in [2b].

The material contained in this release is identical to that contained in the release on IAPWS-IF97, issued by IAPWS in September 1997, except for the basic equation for region 5. The previous basic equation for this region was replaced by a new equation of the same structure. For temperatures between 1073 K and 2273 K, this equation extends the upper range of validity of IAPWS-IF97 in pressure from 10 MPa to 50 MPa. Except for the basic equation for region 5 of IAPWS-IF97, the property calculations are unchanged.

In addition, minor editorial changes to this document, involving correction of typographical errors and updating of references, were made in the 2007 revision, and again in 2009 and 2010. In 2012, the description of the range of validity of the equation for the metastable vapor was clarified.

IAPWS also has a formulation intended for general and scientific use [3].

Further information about this release and other releases issued by IAPWS can be obtained from the Executive Secretary of IAPWS or from http://www.iapws.org.

Contents

1 Nomenclature

Thermodynamic quantities:

c_p	Specific isobaric heat capacity
c_v	Specific isochoric heat capacity
f	Specific Helmholtz free energy
g	Specific Gibbs free energy
h	Specific enthalpy
M	Molar mass
p	Pressure
R	Specific gas constant
R_m	Molar gas constant
s	Specific entropy
T	Absolute temperature [a]
u	Specific internal energy
v	Specific volume
w	Speed of sound
x	General quantity
β	Transformed pressure, Eq. (29a)
γ	Dimensionless Gibbs free energy, $\gamma = g/(RT)$
δ	Reduced density, $\delta = \rho/\rho^*$
Δ	Difference in any quantity
η	Reduced enthalpy, $\eta = h/h^*$
θ	Reduced temperature, $\theta = T/T^*$
ϑ	Transformed temperature, Eq. (29b)
π	Reduced pressure, $\pi = p/p^*$
ρ	Mass density
σ	Reduced entropy, $\sigma = s/s^*$
τ	Inverse reduced temperature, $\tau = T^*/T$
ϕ	Dimensionless Helmholtz free energy, $\phi = f/(RT)$

Superscripts:

o	Ideal-gas part
r	Residual part
*	Reducing quantity
′	Saturated liquid state
″	Saturated vapor state

Subscripts:

c	Critical point
max	Maximum value
RMS	Root-mean-square value
s	Saturation state
t	Triple point
tol	Tolerance of a quantity

Root-mean-square deviation:

$$\Delta x_\mathrm{RMS} = \sqrt{\frac{1}{N}\sum_{n=1}^{N}(\Delta x_n)^2}$$

where Δx_n can be either absolute or percentage difference between the corresponding quantities x; N is the number of Δx_n values (depending on the property, between 10 million and 100 million points are uniformly distributed over the respective range of validity).

[a] Note: T denotes absolute temperature on the International Temperature Scale of 1990.

2 Structure of the Formulation

The IAPWS Industrial Formulation 1997 consists of a set of equations for different regions which cover the following range of validity:

$$273.15\text{ K} \le T \le 1073.15\text{ K} \qquad p \le 100\text{ MPa}$$
$$1073.15\text{ K} < T \le 2273.15\text{ K} \qquad p \le 50\text{ MPa}\,.$$

Figure 1 shows the five regions into which the entire range of validity of IAPWS-IF97 is divided. The boundaries of the regions can be directly taken from Fig. 1 except for the boundary between regions 2 and 3; this boundary is defined by the so-called B23-equation given in Section 4. Both regions 1 and 2 are individually covered by a fundamental equation for the specific Gibbs free energy $g(p,T)$, region 3 by a fundamental equation for the specific Helmholtz free energy $f(\rho,T)$, where ρ is the density, and the saturation curve by a saturation-pressure equation $p_s(T)$. The high-temperature region 5 is also covered by a $g(p,T)$ equation. These five equations, shown in rectangular boxes in Fig. 1, form the so-called *basic equations*.

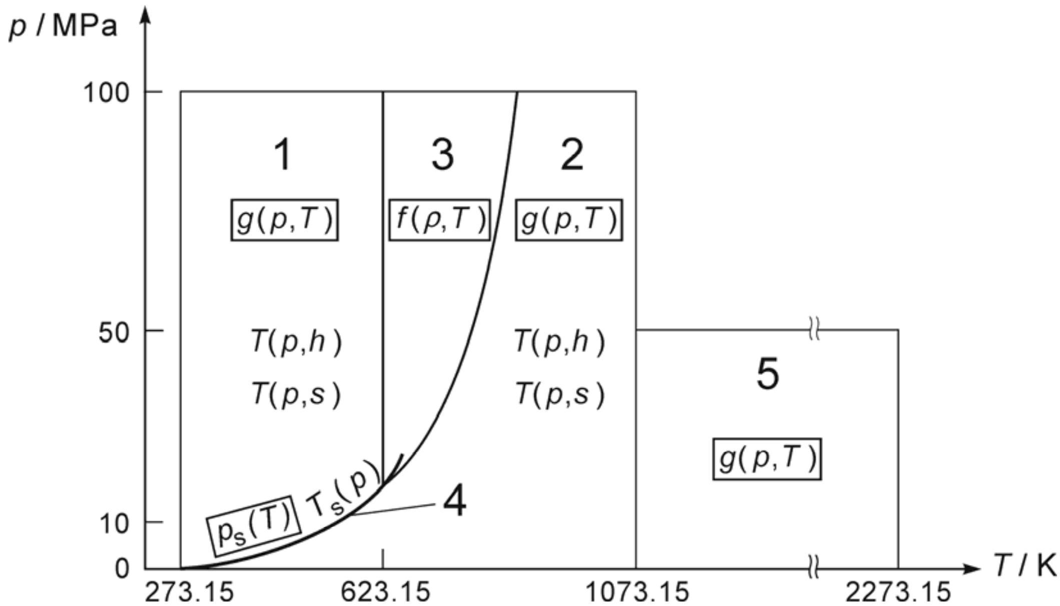

Fig. 1. Regions and equations of IAPWS-IF97.

Regarding the main properties specific volume v, specific enthalpy h, specific isobaric heat capacity c_p, speed of sound w, and saturation pressure p_s, the basic equations represent the corresponding values from the "IAPWS Formulation 1995 for the Thermodynamic Properties of Ordinary Water Substance for General and Scientific Use" [3] (hereafter abbreviated to IAPWS-95) to within the tolerances specified for the development of the corresponding equations; details of these requirements and their fulfillment are given in the comprehensive paper on IAPWS-IF97 [2]. The basic equations for regions 1 and 3 also yield reasonable values for the metastable states close to the stable regions. For region 2 there is a special equation for the metastable-vapor region. Along the region boundaries the corresponding basic equations are consistent with each other within specified tolerances; for details see Section 10.

In addition to the basic equations, for regions 1, 2, and 4 so-called *backward equations* are provided in the forms of $T(p,h)$ and $T(p,s)$ for regions 1 and 2, and $T_s(p)$ for region 4. These backward equations are numerically consistent with the corresponding basic equations and make the calculation of properties as functions of p,h and of p,s for regions 1 and 2, and of p for region 4, extremely fast. In this way, properties such as $T(p,h)$, $h(p,s)$, and $h'(p)$ can be calculated without any iteration from the backward equation alone or by combination with the corresponding basic equation, for example, $h(p,s)$ via the relation $h(p,T(p,s))$. As a consequence, the calculation of the industrially most important properties is on average more than five times faster than the corresponding calculation with IFC-67; for details see Section 11.

The estimates of uncertainty of the most relevant properties calculated from the corresponding equations of IAPWS-IF97 are summarized in Section 12.

3 Reference Constants

The specific gas constant of ordinary water used for this formulation is

$$R = 0.461\,526 \text{ kJ kg}^{-1}\text{ K}^{-1}. \tag{1}$$

This value results from the recommended values of the molar gas constant [4], and the molar mass of ordinary water [5, 6]. The values of the critical parameters

$$T_c = 647.096 \text{ K} \tag{2}$$

$$p_c = 22.064 \text{ MPa} \tag{3}$$

$$\rho_c = 322 \text{ kg m}^{-3} \tag{4}$$

are from the corresponding IAPWS release [7].

4 Auxiliary Equation for the Boundary between Regions 2 and 3

The boundary between regions 2 and 3 (see Fig. 1) is defined by the following simple quadratic pressure-temperature relation, the B23-equation

$$\pi = n_1 + n_2\theta + n_3\theta^2 \tag{5}$$

where $\pi = p/p^*$ and $\theta = T/T^*$ with $p^* = 1$ MPa and $T^* = 1$ K. The coefficients n_1 to n_3 of Eq. (5) are listed in Table 1. Equation (5) roughly describes an isentropic line; the entropy values along this boundary line are between $s = 5.047$ kJ kg^{-1} K^{-1} and $s = 5.261$ kJ kg^{-1} K^{-1}.

Alternatively Eq. (5) can be expressed explicitly in temperature as

$$\theta = n_4 + \left[\left(\pi - n_5 \right) / n_3 \right]^{1/2} \quad , \tag{6}$$

with θ and π defined for Eq. (5) and the coefficients n_3 to n_5 listed in Table 1. Equations (5) and (6) cover the range from 623.15 K at a pressure of 16.5292 MPa to 863.15 K at 100 MPa.

Table 1. Numerical values of the coefficients of the B23-equation, Eqs. (5) and (6), for defining the boundary between regions 2 and 3

i	n_i	i	n_i
1	$0.348\,051\,856\,289\,69 \times 10^{3}$	4	$0.572\,544\,598\,627\,46 \times 10^{3}$
2	$-0.116\,718\,598\,799\,75 \times 10^{1}$	5	$0.139\,188\,397\,788\,70 \times 10^{2}$
3	$0.101\,929\,700\,393\,26 \times 10^{-2}$		

For *computer-program verification*, Eqs. (5) and (6) must meet the following *T*-*p* point:
$T = 0.623\,150\,000 \times 10^3$ K, $p = 0.165\,291\,643 \times 10^2$ MPa.

5 Equations for Region 1

This section contains all details relevant for the use of the basic and backward equations of region 1 of IAPWS-IF97. Information about the consistency of the basic equation of this region with the basic equations of regions 3 and 4 along the corresponding region boundaries is summarized in Section 10. The results of computing-time comparisons between IAPWS-IF97 and IFC-67 are given in Section 11. The estimates of uncertainty of the most relevant properties can be found in Section 12.

5.1 Basic Equation

The basic equation for this region is a fundamental equation for the specific Gibbs free energy g. This equation is expressed in dimensionless form, $\gamma = g/(RT)$, and reads

$$\frac{g(p,T)}{RT} = \gamma\left(\pi, \tau\right) = \sum_{i=1}^{34} n_i \left(7.1 - \pi\right)^{I_i} \left(\tau - 1.222\right)^{J_i} , \tag{7}$$

where $\pi = p/p^*$ and $\tau = T^*/T$ with $p^* = 16.53$ MPa and $T^* = 1386$ K; R is given by Eq. (1). The coefficients n_i and exponents I_i and J_i of Eq. (7) are listed in Table 2.

All thermodynamic properties can be derived from Eq. (7) by using the appropriate combinations of the dimensionless Gibbs free energy and its derivatives. Relations between the relevant thermodynamic properties and γ and its derivatives are summarized in Table 3. All required derivatives of the dimensionless Gibbs free energy are explicitly given in Table 4.

Since the 5th International Conference on the Properties of Steam in London in 1956, the specific internal energy and the specific entropy of the saturated liquid at the triple point have been set equal to zero:

$$u'_{\mathrm{t}} = 0 \quad ; \quad s'_{\mathrm{t}} = 0 \ . \tag{8}$$

In order to meet this condition at the temperature and pressure of the triple point

$$T_{\mathrm{t}} = 273.16 \text{ K [8]} \qquad p_{\mathrm{t}} = 611.657 \text{ Pa [9]} \ , \tag{9}$$

the coefficients n_3 and n_4 in Eq. (7) have been adjusted accordingly. As a consequence, Eq. (7) yields for the specific enthalpy of the saturated liquid at the triple point

$$h'_{\mathrm{t}} = 0.611\ 783 \text{ J kg}^{-1} \ . \tag{10}$$

Table 2. Numerical values of the coefficients and exponents of the dimensionless Gibbs free energy for region 1, Eq. (7)

i	I_i	J_i	n_i	i	I_i	J_i	n_i
1	0	−2	0.146 329 712 131 67	18	2	3	$-0.441\ 418\ 453\ 308\ 46 \times 10^{-5}$
2	0	−1	−0.845 481 871 691 14	19	2	17	$-0.726\ 949\ 962\ 975\ 94 \times 10^{-15}$
3	0	0	$-0.375\ 636\ 036\ 720\ 40 \times 10^{1}$	20	3	−4	$-0.316\ 796\ 448\ 450\ 54 \times 10^{-4}$
4	0	1	$0.338\ 551\ 691\ 683\ 85 \times 10^{1}$	21	3	0	$-0.282\ 707\ 979\ 853\ 12 \times 10^{-5}$
5	0	2	−0.957 919 633 878 72	22	3	6	$-0.852\ 051\ 281\ 201\ 03 \times 10^{-9}$
6	0	3	0.157 720 385 132 28	23	4	−5	$-0.224\ 252\ 819\ 080\ 00 \times 10^{-5}$
7	0	4	$-0.166\ 164\ 171\ 995\ 01 \times 10^{-1}$	24	4	−2	$-0.651\ 712\ 228\ 956\ 01 \times 10^{-6}$
8	0	5	$0.812\ 146\ 299\ 835\ 68 \times 10^{-3}$	25	4	10	$-0.143\ 417\ 299\ 379\ 24 \times 10^{-12}$
9	1	−9	$0.283\ 190\ 801\ 238\ 04 \times 10^{-3}$	26	5	−8	$-0.405\ 169\ 968\ 601\ 17 \times 10^{-6}$
10	1	−7	$-0.607\ 063\ 015\ 658\ 74 \times 10^{-3}$	27	8	−11	$-0.127\ 343\ 017\ 416\ 41 \times 10^{-8}$
11	1	−1	$-0.189\ 900\ 682\ 184\ 19 \times 10^{-1}$	28	8	−6	$-0.174\ 248\ 712\ 306\ 34 \times 10^{-9}$
12	1	0	$-0.325\ 297\ 487\ 705\ 05 \times 10^{-1}$	29	21	−29	$-0.687\ 621\ 312\ 955\ 31 \times 10^{-18}$
13	1	1	$-0.218\ 417\ 171\ 754\ 14 \times 10^{-1}$	30	23	−31	$0.144\ 783\ 078\ 285\ 21 \times 10^{-19}$
14	1	3	$-0.528\ 383\ 579\ 699\ 30 \times 10^{-4}$	31	29	−38	$0.263\ 357\ 816\ 627\ 95 \times 10^{-22}$
15	2	−3	$-0.471\ 843\ 210\ 732\ 67 \times 10^{-3}$	32	30	−39	$-0.119\ 476\ 226\ 400\ 71 \times 10^{-22}$
16	2	0	$-0.300\ 017\ 807\ 930\ 26 \times 10^{-3}$	33	31	−40	$0.182\ 280\ 945\ 814\ 04 \times 10^{-23}$
17	2	1	$0.476\ 613\ 939\ 069\ 87 \times 10^{-4}$	34	32	−41	$-0.935\ 370\ 872\ 924\ 58 \times 10^{-25}$

Table 3. Relations of thermodynamic properties to the dimensionless Gibbs free energy γ and its derivatives[a] when using Eq. (7)

Property	Relation
Specific volume $v = (\partial g/\partial p)_T$	$v(\pi,\tau)\dfrac{p}{RT} = \pi\gamma_\pi$
Specific internal energy $u = g - T(\partial g/\partial T)_p - p(\partial g/\partial p)_T$	$\dfrac{u(\pi,\tau)}{RT} = \tau\gamma_\tau - \pi\gamma_\pi$
Specific entropy $s = -(\partial g/\partial T)_p$	$\dfrac{s(\pi,\tau)}{R} = \tau\gamma_\tau - \gamma$
Specific enthalpy $h = g - T(\partial g/\partial T)_p$	$\dfrac{h(\pi,\tau)}{RT} = \tau\gamma_\tau$
Specific isobaric heat capacity $c_p = (\partial h/\partial T)_p$	$\dfrac{c_p(\pi,\tau)}{R} = -\tau^2\gamma_{\tau\tau}$
Specific isochoric heat capacity $c_v = (\partial u/\partial T)_v$	$\dfrac{c_v(\pi,\tau)}{R} = -\tau^2\gamma_{\tau\tau} + \dfrac{(\gamma_\pi - \tau\gamma_{\pi\tau})^2}{\gamma_{\pi\pi}}$
Speed of sound $w = v\left[-(\partial p/\partial v)_s\right]^{1/2}$	$\dfrac{w^2(\pi,\tau)}{RT} = \dfrac{\gamma_\pi^2}{\dfrac{(\gamma_\pi - \tau\gamma_{\pi\tau})^2}{\tau^2\gamma_{\tau\tau}} - \gamma_{\pi\pi}}$

[a] $\gamma_\pi = \left[\dfrac{\partial\gamma}{\partial\pi}\right]_\tau$, $\gamma_{\pi\pi} = \left[\dfrac{\partial^2\gamma}{\partial\pi^2}\right]_\tau$, $\gamma_\tau = \left[\dfrac{\partial\gamma}{\partial\tau}\right]_\pi$, $\gamma_{\tau\tau} = \left[\dfrac{\partial^2\gamma}{\partial\tau^2}\right]_\pi$, $\gamma_{\pi\tau} = \left[\dfrac{\partial^2\gamma}{\partial\pi\partial\tau}\right]$

Table 4. The dimensionless Gibbs free energy γ and its derivatives[a] according to Eq. (7)

$$\gamma = \sum_{i=1}^{34} n_i (7.1-\pi)^{I_i} (\tau - 1.222)^{J_i}$$

$$\gamma_\pi = \sum_{i=1}^{34} -n_i I_i (7.1-\pi)^{I_i - 1} (\tau - 1.222)^{J_i} \qquad \gamma_{\pi\pi} = \sum_{i=1}^{34} n_i I_i (I_i - 1)(7.1-\pi)^{I_i - 2} (\tau - 1.222)^{J_i}$$

$$\gamma_\tau = \sum_{i=1}^{34} n_i (7.1-\pi)^{I_i} J_i (\tau - 1.222)^{J_i - 1} \qquad \gamma_{\tau\tau} = \sum_{i=1}^{34} n_i (7.1-\pi)^{I_i} J_i (J_i - 1)(\tau - 1.222)^{J_i - 2}$$

$$\gamma_{\pi\tau} = \sum_{i=1}^{34} -n_i I_i (7.1-\pi)^{I_i - 1} J_i (\tau - 1.222)^{J_i - 1}$$

[a] $\gamma_\pi = \left[\dfrac{\partial\gamma}{\partial\pi}\right]_\tau$, $\gamma_{\pi\pi} = \left[\dfrac{\partial^2\gamma}{\partial\pi^2}\right]_\tau$, $\gamma_\tau = \left[\dfrac{\partial\gamma}{\partial\tau}\right]_\pi$, $\gamma_{\tau\tau} = \left[\dfrac{\partial^2\gamma}{\partial\tau^2}\right]_\pi$, $\gamma_{\pi\tau} = \left[\dfrac{\partial^2\gamma}{\partial\pi\partial\tau}\right]$

Range of validity

Equation (7) covers region 1 of IAPWS-IF97 defined by the following range of temperature and pressure; see Fig. 1:

$$273.15 \text{ K} \le T \le 623.15 \text{ K} \qquad p_s(T) \le p \le 100 \text{ MPa} .$$

In addition to the properties in the stable single-phase liquid region, Eq. (7) also yields reasonable values in the metastable superheated-liquid region close to the saturated liquid line.

Note: For temperatures between 273.15 K and 273.16 K, the part of the range of validity between the pressures on the melting line [10] and on the saturation-pressure line, Eq. (30), corresponds to metastable states.

Computer-program verification

To assist the user in computer-program verification of Eq. (7), Table 5 contains test values of the most relevant properties.

Table 5. Thermodynamic property values calculated from Eq. (7) for selected values of T and p [a]

	T = 300 K, p = 3 MPa	T = 300 K, p = 80 MPa	T = 500 K, p = 3 MPa
$v/(\text{m}^3\ \text{kg}^{-1})$	$0.100\,215\,168 \times 10^{-2}$	$0.971\,180\,894 \times 10^{-3}$	$0.120\,241\,800 \times 10^{-2}$
$h/(\text{kJ kg}^{-1})$	$0.115\,331\,273 \times 10^{3}$	$0.184\,142\,828 \times 10^{3}$	$0.975\,542\,239 \times 10^{3}$
$u/(\text{kJ kg}^{-1})$	$0.112\,324\,818 \times 10^{3}$	$0.106\,448\,356 \times 10^{3}$	$0.971\,934\,985 \times 10^{3}$
$s/(\text{kJ kg}^{-1}\ \text{K}^{-1})$	$0.392\,294\,792$	$0.368\,563\,852$	$0.258\,041\,912 \times 10^{1}$
$c_p/(\text{kJ kg}^{-1}\ \text{K}^{-1})$	$0.417\,301\,218 \times 10^{1}$	$0.401\,008\,987 \times 10^{1}$	$0.465\,580\,682 \times 10^{1}$
$w/(\text{m s}^{-1})$	$0.150\,773\,921 \times 10^{4}$	$0.163\,469\,054 \times 10^{4}$	$0.124\,071\,337 \times 10^{4}$

[a] It is recommended to verify programmed functions using 8 byte real values for all three combinations of T and p given in this table.

5.2 Backward Equations

For the calculation of properties as function of p,h or of p,s without any iteration, the two backward equations require extremely good numerical consistency with the basic equation. The exact requirements for these numerical consistencies were obtained from comprehensive test calculations for several characteristic power cycles. The result of these investigations, namely the assignment of the tolerable numerical inconsistencies between the basic equation, Eq. (7), and the corresponding backward equations, is given in Eqs. (12) and (14), respectively.

5.2.1 The Backward Equation $T(p,h)$

The backward equation $T(p,h)$ for region 1 has the following dimensionless form:

$$\frac{T(p,h)}{T^*} = \theta(\pi,\eta) = \sum_{i=1}^{20} n_i \pi^{I_i} (\eta + 1)^{J_i} \quad , \tag{11}$$

where $\theta = T/T^*$, $\pi = p/p^*$, and $\eta = h/h^*$ with $T^* = 1\ \mathrm{K}$, $p^* = 1\ \mathrm{MPa}$, and $h^* = 2500\ \mathrm{kJ\ kg^{-1}}$. The coefficients n_i and exponents I_i and J_i of Eq. (11) are listed in Table 6.

Table 6. Numerical values of the coefficients and exponents of the backward equation $T(p,h)$ for region 1, Eq. (11)

i	I_i	J_i	n_i	i	I_i	J_i	n_i
1	0	0	$-0.238\,724\,899\,245\,21 \times 10^{3}$	11	1	4	$-0.659\,647\,494\,236\,38 \times 10^{1}$
2	0	1	$0.404\,211\,886\,379\,45 \times 10^{3}$	12	1	10	$0.939\,654\,008\,783\,63 \times 10^{-2}$
3	0	2	$0.113\,497\,468\,817\,18 \times 10^{3}$	13	1	32	$0.115\,736\,475\,053\,40 \times 10^{-6}$
4	0	6	$-0.584\,576\,160\,480\,39 \times 10^{1}$	14	2	10	$-0.258\,586\,412\,820\,73 \times 10^{-4}$
5	0	22	$-0.152\,854\,824\,131\,40 \times 10^{-3}$	15	2	32	$-0.406\,443\,630\,847\,99 \times 10^{-8}$
6	0	32	$-0.108\,667\,076\,953\,77 \times 10^{-5}$	16	3	10	$0.664\,561\,861\,916\,35 \times 10^{-7}$
7	1	0	$-0.133\,917\,448\,726\,02 \times 10^{2}$	17	3	32	$0.806\,707\,341\,030\,27 \times 10^{-10}$
8	1	1	$0.432\,110\,391\,835\,59 \times 10^{2}$	18	4	32	$-0.934\,777\,712\,139\,47 \times 10^{-12}$
9	1	2	$-0.540\,100\,671\,705\,06 \times 10^{2}$	19	5	32	$0.582\,654\,420\,206\,01 \times 10^{-14}$
10	1	3	$0.305\,358\,922\,039\,16 \times 10^{2}$	20	6	32	$-0.150\,201\,859\,535\,03 \times 10^{-16}$

Range of validity

Equation (11) covers the same range of validity as the basic equation, Eq. (7), except for the metastable region (superheated liquid), where Eq. (11) is not valid.

Numerical consistency with the basic equation

For ten million random pairs of p and h covering the entire region 1, the differences ΔT between temperatures from Eq. (11) and from Eq. (7) were calculated and the absolute maximum difference $|\Delta T|_{\mathrm{max}}$ and the root-mean-square difference ΔT_{RMS} were determined. These actual inconsistency values and the tolerated value $|\Delta T|_{\mathrm{tol}}$ (see the beginning of Section 5.2) amount to:

$$|\Delta T|_{\mathrm{tol}} = 25\ \mathrm{mK} \quad ; \quad \Delta T_{\mathrm{RMS}} = 13.4\ \mathrm{mK} \quad ; \quad |\Delta T|_{\mathrm{max}} = 23.6\ \mathrm{mK}\ . \tag{12}$$

Computer-program verification

To assist the user in computer-program verification of Eq. (11), Table 7 contains the corresponding test values.

Table 7. Temperature values calculated from Eq. (11) for selected values of p and h[a]

p/MPa	h/(kJ kg^{-1})	T/K
3	500	$0.391\,798\,509 \times 10^3$
80	500	$0.378\,108\,626 \times 10^3$
80	1500	$0.611\,041\,229 \times 10^3$

[a] It is recommended to verify the programmed equation (8 byte real values) for all three combinations of p and h given in this table.

5.2.2 The Backward Equation $T(p,s)$

The backward equation $T(p,s)$ for region 1 has the following dimensionless form:

$$\frac{T(p,s)}{T^*} = \theta(\pi,\sigma) = \sum_{i=1}^{20} n_i\, \pi^{I_i} (\sigma + 2)^{J_i} , \tag{13}$$

where $\theta = T/T^*$, $\pi = p/p^*$, and $\sigma = s/s^*$ with $T^* = 1$ K, $p^* = 1$ MPa, and $s^* = 1$ kJ kg^{-1} K^{-1}. The coefficients n_i and exponents I_i and J_i of Eq. (13) are listed in Table 8.

Table 8. Numerical values of the coefficients and exponents of the backward equation $T(p,s)$ for region 1, Eq. (13)

i	I_i	J_i	n_i	i	I_i	J_i	n_i
1	0	0	$0.174\,782\,680\,583\,07 \times 10^{3}$	11	1	12	$0.356\,721\,106\,073\,66 \times 10^{-9}$
2	0	1	$0.348\,069\,308\,928\,73 \times 10^{2}$	12	1	31	$0.173\,324\,969\,948\,95 \times 10^{-23}$
3	0	2	$0.652\,925\,849\,784\,55 \times 10^{1}$	13	2	0	$0.566\,089\,006\,548\,37 \times 10^{-3}$
4	0	3	$0.330\,399\,817\,754\,89$	14	2	1	$-0.326\,354\,831\,397\,17 \times 10^{-3}$
5	0	11	$-0.192\,813\,829\,231\,96 \times 10^{-6}$	15	2	2	$0.447\,782\,866\,906\,32 \times 10^{-4}$
6	0	31	$-0.249\,091\,972\,445\,73 \times 10^{-22}$	16	2	9	$-0.513\,221\,569\,085\,07 \times 10^{-9}$
7	1	0	$-0.261\,076\,364\,893\,32$	17	2	31	$-0.425\,226\,570\,422\,07 \times 10^{-25}$
8	1	1	$0.225\,929\,659\,815\,86$	18	3	10	$0.264\,004\,413\,606\,89 \times 10^{-12}$
9	1	2	$-0.642\,564\,633\,952\,26 \times 10^{-1}$	19	3	32	$0.781\,246\,004\,597\,23 \times 10^{-28}$
10	1	3	$0.788\,762\,892\,705\,26 \times 10^{-2}$	20	4	32	$-0.307\,321\,999\,036\,68 \times 10^{-30}$

Range of validity

Equation (13) covers the same range of validity as the basic equation, Eq. (7), except for the metastable region (superheated liquid), where Eq. (13) is not valid.

Numerical consistency with the basic equation

For ten million random pairs of p and s covering the entire region 1, the differences ΔT between temperatures from Eq. (13) and from Eq. (7) were calculated and the absolute maximum difference $|\Delta T|_{max}$ and the root-mean-square difference ΔT_{RMS} were determined. These actual differences and the tolerated value $|\Delta T|_{tol}$ (see the beginning of Section 5.2) amount to:

$$|\Delta T|_{tol} = 25\text{ mK} \quad ; \quad \Delta T_{RMS} = 5.8\text{ mK} \quad ; \quad |\Delta T|_{max} = 21.8\text{ mK} . \tag{14}$$

Computer-program verification

To assist the user in computer-program verification of Eq. (13), Table 9 contains the corresponding test values.

Table 9. Temperature values calculated from Eq. (13) for selected values of p and s [a]

p/MPa	s/(kJ kg^{-1} K^{-1})	T/K
3	0.5	$0.307\,842\,258 \times 10^3$
80	0.5	$0.309\,979\,785 \times 10^3$
80	3	$0.565\,899\,909 \times 10^3$

[a] It is recommended to verify the programmed equation using 8 byte real values for all three combinations of p and s given in this table.

6 Equations for Region 2

This section contains all details relevant for the use of the basic and backward equations of region 2 of IAPWS-IF97. Information about the consistency of the basic equation of this region with the basic equations of regions 3, 4 and 5 along the corresponding region boundaries is summarized in Section 10. The auxiliary equation for defining the boundary between regions 2 and 3 is given in Section 4. Section 11 contains the results of computing-time comparisons between IAPWS-IF97 and IFC-67. The estimates of uncertainty of the most relevant properties can be found in Section 12.

6.1 Basic Equation

The basic equation for this region is a fundamental equation for the specific Gibbs free energy g. This equation is expressed in dimensionless form, $\gamma = g/(RT)$, and is separated into two parts, an ideal-gas part γ^{o} and a residual part γ^{r}, so that

$$\frac{g(p,T)}{RT} = \gamma(\pi,\tau) = \gamma^{\mathrm{o}}(\pi,\tau) + \gamma^{\mathrm{r}}(\pi,\tau) \ , \tag{15}$$

where $\pi = p/p^*$ and $\tau = T^*/T$ with R given by Eq. (1).

The equation for the ideal-gas part γ^{o} of the dimensionless Gibbs free energy reads

$$\gamma^{\mathrm{o}} = \ln \pi + \sum_{i=1}^{9} n_i^{\mathrm{o}} \tau^{J_i^{\mathrm{o}}} \ , \tag{16}$$

where $\pi = p/p^*$ and $\tau = T^*/T$ with $p^* = 1$ MPa and $T^* = 540$ K. The coefficients n_1^{o} and n_2^{o} were adjusted in such a way that the values for the specific internal energy and specific entropy in the ideal-gas state relate to Eq. (8). Table 10 contains the coefficients n_i^{o} and exponents J_i^{o} of Eq. (16).

Table 10. Numerical values of the coefficients and exponents of the ideal-gas part γ^{o} of the dimensionless Gibbs free energy for region 2, Eq. (16)[a]

i	J_i^{o}	n_i^{o}	i	J_i^{o}	n_i^{o}
1[a]	0	$-0.969\,276\,865\,002\,17 \times 10^{1}$	6	-2	$0.142\,408\,191\,714\,44 \times 10^{1}$
2[a]	1	$0.100\,866\,559\,680\,18 \times 10^{2}$	7	-1	$-0.438\,395\,113\,194\,50 \times 10^{1}$
3	-5	$-0.560\,879\,112\,830\,20 \times 10^{-2}$	8	2	$-0.284\,086\,324\,607\,72$
4	-4	$0.714\,527\,380\,814\,55 \times 10^{-1}$	9	3	$0.212\,684\,637\,533\,07 \times 10^{-1}$
5	-3	$-0.407\,104\,982\,239\,28$			

[a] If Eq. (16) is incorporated into Eq. (18), instead of the values for n_1^{o} and n_2^{o} given above, the following values for these two coefficients must be used: $n_1^{\mathrm{o}} = -0.969\,372\,683\,930\,49 \times 10^{1}$, $n_2^{\mathrm{o}} = 0.100\,872\,759\,700\,06 \times 10^{2}$.

The form of the residual part γ^{r} of the dimensionless Gibbs free energy is as follows:

$$\gamma^{\mathrm{r}} = \sum_{i=1}^{43} n_i \, \pi^{I_i} \left(\tau - 0.5\right)^{J_i} \ , \tag{17}$$

where $\pi = p/p^*$ and $\tau = T^*/T$ with $p^* = 1$ MPa and $T^* = 540$ K. The coefficients n_i and exponents I_i and J_i of Eq. (17) are listed in Table 11.

Table 11. Numerical values of the coefficients and exponents of the residual part γ^{r} of the dimensionless Gibbs free energy for region 2, Eq. (17)

i	I_i	J_i	n_i
1	1	0	$-0.177\,317\,424\,732\,13 \times 10^{-2}$
2	1	1	$-0.178\,348\,622\,923\,58 \times 10^{-1}$
3	1	2	$-0.459\,960\,136\,963\,65 \times 10^{-1}$
4	1	3	$-0.575\,812\,590\,834\,32 \times 10^{-1}$
5	1	6	$-0.503\,252\,787\,279\,30 \times 10^{-1}$
6	2	1	$-0.330\,326\,416\,702\,03 \times 10^{-4}$
7	2	2	$-0.189\,489\,875\,163\,15 \times 10^{-3}$
8	2	4	$-0.393\,927\,772\,433\,55 \times 10^{-2}$
9	2	7	$-0.437\,972\,956\,505\,73 \times 10^{-1}$
10	2	36	$-0.266\,745\,479\,140\,87 \times 10^{-4}$
11	3	0	$0.204\,817\,376\,923\,09 \times 10^{-7}$
12	3	1	$0.438\,706\,672\,844\,35 \times 10^{-6}$
13	3	3	$-0.322\,776\,772\,385\,70 \times 10^{-4}$
14	3	6	$-0.150\,339\,245\,421\,48 \times 10^{-2}$
15	3	35	$-0.406\,682\,535\,626\,49 \times 10^{-1}$
16	4	1	$-0.788\,473\,095\,593\,67 \times 10^{-9}$
17	4	2	$0.127\,907\,178\,522\,85 \times 10^{-7}$
18	4	3	$0.482\,253\,727\,185\,07 \times 10^{-6}$
19	5	7	$0.229\,220\,763\,376\,61 \times 10^{-5}$
20	6	3	$-0.167\,147\,664\,510\,61 \times 10^{-10}$
21	6	16	$-0.211\,714\,723\,213\,55 \times 10^{-2}$
22	6	35	$-0.238\,957\,419\,341\,04 \times 10^{2}$
23	7	0	$-0.590\,595\,643\,242\,70 \times 10^{-17}$
24	7	11	$-0.126\,218\,088\,991\,01 \times 10^{-5}$
25	7	25	$-0.389\,468\,424\,357\,39 \times 10^{-1}$
26	8	8	$0.112\,562\,113\,604\,59 \times 10^{-10}$
27	8	36	$-0.823\,113\,408\,979\,98 \times 10^{1}$
28	9	13	$0.198\,097\,128\,020\,88 \times 10^{-7}$
29	10	4	$0.104\,069\,652\,101\,74 \times 10^{-18}$
30	10	10	$-0.102\,347\,470\,959\,29 \times 10^{-12}$
31	10	14	$-0.100\,181\,793\,795\,11 \times 10^{-8}$
32	16	29	$-0.808\,829\,086\,469\,85 \times 10^{-10}$
33	16	50	$0.106\,930\,318\,794\,09$
34	18	57	$-0.336\,622\,505\,741\,71$
35	20	20	$0.891\,858\,453\,554\,21 \times 10^{-24}$
36	20	35	$0.306\,293\,168\,762\,32 \times 10^{-12}$
37	20	48	$-0.420\,024\,676\,982\,08 \times 10^{-5}$
38	21	21	$-0.590\,560\,296\,856\,39 \times 10^{-25}$
39	22	53	$0.378\,269\,476\,134\,57 \times 10^{-5}$
40	23	39	$-0.127\,686\,089\,346\,81 \times 10^{-14}$
41	24	26	$0.730\,876\,105\,950\,61 \times 10^{-28}$
42	24	40	$0.554\,147\,153\,507\,78 \times 10^{-16}$
43	24	58	$-0.943\,697\,072\,412\,10 \times 10^{-6}$

All thermodynamic properties can be derived from Eq. (15) by using the appropriate combinations of the ideal-gas part γ^{o}, Eq. (16), and the residual part γ^{r}, Eq. (17), of the dimensionless Gibbs free energy and their derivatives. Relations between the relevant thermodynamic properties and γ^{o} and γ^{r} and their derivatives are summarized in Table 12. All required derivatives of the ideal-gas part and of the residual part of the dimensionless Gibbs free energy are explicitly given in Table 13 and Table 14, respectively.

Table 12. Relations of thermodynamic properties to the ideal-gas part γ^{o} and the residual part γ^{r} of the dimensionless Gibbs free energy and their derivatives [a] when using Eq. (15) or Eq. (18)

Property	Relation
Specific volume $v = (\partial g/\partial p)_T$	$v(\pi,\tau)\dfrac{p}{RT} = \pi\left(\gamma_\pi^{\mathrm{o}} + \gamma_\pi^{\mathrm{r}}\right)$
Specific internal energy $u = g - T(\partial g/\partial T)_p - p(\partial g/\partial p)_T$	$\dfrac{u(\pi,\tau)}{RT} = \tau\left(\gamma_\tau^{\mathrm{o}} + \gamma_\tau^{\mathrm{r}}\right) - \pi\left(\gamma_\pi^{\mathrm{o}} + \gamma_\pi^{\mathrm{r}}\right)$
Specific entropy $s = -(\partial g/\partial T)_p$	$\dfrac{s(\pi,\tau)}{R} = \tau\left(\gamma_\tau^{\mathrm{o}} + \gamma_\tau^{\mathrm{r}}\right) - \left(\gamma^{\mathrm{o}} + \gamma^{\mathrm{r}}\right)$
Specific enthalpy $h = g - T(\partial g/\partial T)_p$	$\dfrac{h(\pi,\tau)}{RT} = \tau\left(\gamma_\tau^{\mathrm{o}} + \gamma_\tau^{\mathrm{r}}\right)$
Specific isobaric heat capacity $c_p = (\partial h/\partial T)_p$	$\dfrac{c_p(\pi,\tau)}{R} = -\tau^2\left(\gamma_{\tau\tau}^{\mathrm{o}} + \gamma_{\tau\tau}^{\mathrm{r}}\right)$
Specific isochoric heat capacity $c_v = (\partial u/\partial T)_v$	$\dfrac{c_v(\pi,\tau)}{R} = -\tau^2\left(\gamma_{\tau\tau}^{\mathrm{o}} + \gamma_{\tau\tau}^{\mathrm{r}}\right) - \dfrac{(1+\pi\gamma_\pi^{\mathrm{r}} - \tau\pi\gamma_{\pi\tau}^{\mathrm{r}})^2}{1-\pi^2\gamma_{\pi\pi}^{\mathrm{r}}}$
Speed of sound $w = v\left[-(\partial p/\partial v)_s\right]^{1/2}$	$\dfrac{w^2(\pi,\tau)}{RT} = \dfrac{1+2\pi\gamma_\pi^{\mathrm{r}} + \pi^2\gamma_\pi^{\mathrm{r}\,2}}{\left(1-\pi^2\gamma_{\pi\pi}^{\mathrm{r}}\right) + \dfrac{\left(1+\pi\gamma_\pi^{\mathrm{r}} - \tau\pi\gamma_{\pi\tau}^{\mathrm{r}}\right)^2}{\tau^2\left(\gamma_{\tau\tau}^{\mathrm{o}} + \gamma_{\tau\tau}^{\mathrm{r}}\right)}}$

[a] $\gamma_\pi^{\mathrm{r}} = \left[\dfrac{\partial\gamma^{\mathrm{r}}}{\partial\pi}\right]_\tau$, $\gamma_{\pi\pi}^{\mathrm{r}} = \left[\dfrac{\partial^2\gamma^{\mathrm{r}}}{\partial\pi^2}\right]_\tau$, $\gamma_\tau^{\mathrm{r}} = \left[\dfrac{\partial\gamma^{\mathrm{r}}}{\partial\tau}\right]_\pi$, $\gamma_{\tau\tau}^{\mathrm{r}} = \left[\dfrac{\partial^2\gamma^{\mathrm{r}}}{\partial\tau^2}\right]_\pi$, $\gamma_{\pi\tau}^{\mathrm{r}} = \left[\dfrac{\partial^2\gamma^{\mathrm{r}}}{\partial\pi\partial\tau}\right]$,

$\gamma_\tau^{\mathrm{o}} = \left[\dfrac{\partial\gamma^{\mathrm{o}}}{\partial\tau}\right]_\pi$, $\gamma_{\tau\tau}^{\mathrm{o}} = \left[\dfrac{\partial^2\gamma^{\mathrm{o}}}{\partial\tau^2}\right]_\pi$

Table 13. The ideal-gas part γ^{o} of the dimensionless Gibbs free energy and its derivatives [a] according to Eq. (16)

$$\gamma^{\mathrm{o}} = \ln\pi + \sum_{i=1}^{9} n_i^{\mathrm{o}} \tau^{J_i^{\mathrm{o}}}$$

$$\gamma_\pi^{\mathrm{o}} = 1/\pi + 0$$

$$\gamma_{\pi\pi}^{\mathrm{o}} = -1/\pi^2 + 0$$

$$\gamma_\tau^{\mathrm{o}} = 0 + \sum_{i=1}^{9} n_i^{\mathrm{o}} J_i^{\mathrm{o}} \tau^{J_i^{\mathrm{o}}-1}$$

$$\gamma_{\tau\tau}^{\mathrm{o}} = 0 + \sum_{i=1}^{9} n_i^{\mathrm{o}} J_i^{\mathrm{o}} \left(J_i^{\mathrm{o}}-1\right) \tau^{J_i^{\mathrm{o}}-2}$$

$$\gamma_{\pi\tau}^{\mathrm{o}} = 0 + 0$$

[a] $\gamma_\pi^{\mathrm{o}} = \left[\frac{\partial \gamma^{\mathrm{o}}}{\partial \pi}\right]_\tau$, $\gamma_{\pi\pi}^{\mathrm{o}} = \left[\frac{\partial^2 \gamma^{\mathrm{o}}}{\partial \pi^2}\right]_\tau$, $\gamma_\tau^{\mathrm{o}} = \left[\frac{\partial \gamma^{\mathrm{o}}}{\partial \tau}\right]_\pi$, $\gamma_{\tau\tau}^{\mathrm{o}} = \left[\frac{\partial^2 \gamma^{\mathrm{o}}}{\partial \tau^2}\right]_\pi$, $\gamma_{\pi\tau}^{\mathrm{o}} = \left[\frac{\partial^2 \gamma^{\mathrm{o}}}{\partial \pi \partial \tau}\right]$

Table 14. The residual part γ^{r} of the dimensionless Gibbs free energy and its derivatives [a] according to Eq. (17)

$$\gamma^{\mathrm{r}} = \sum_{i=1}^{43} n_i \, \pi^{I_i} \left(\tau - 0.5\right)^{J_i}$$

$$\gamma_\pi^{\mathrm{r}} = \sum_{i=1}^{43} n_i \, I_i \, \pi^{I_i-1} \left(\tau - 0.5\right)^{J_i}$$

$$\gamma_{\pi\pi}^{\mathrm{r}} = \sum_{i=1}^{43} n_i \, I_i \left(I_i - 1\right) \pi^{I_i-2} \left(\tau - 0.5\right)^{J_i}$$

$$\gamma_\tau^{\mathrm{r}} = \sum_{i=1}^{43} n_i \, \pi^{I_i} J_i \left(\tau - 0.5\right)^{J_i-1}$$

$$\gamma_{\tau\tau}^{\mathrm{r}} = \sum_{i=1}^{43} n_i \, \pi^{I_i} J_i \left(J_i - 1\right) \left(\tau - 0.5\right)^{J_i-2}$$

$$\gamma_{\pi\tau}^{\mathrm{r}} = \sum_{i=1}^{43} n_i \, I_i \, \pi^{I_i-1} J_i \left(\tau - 0.5\right)^{J_i-1}$$

[a] $\gamma_\pi^{\mathrm{r}} = \left[\frac{\partial \gamma^{\mathrm{r}}}{\partial \pi}\right]_\tau$, $\gamma_{\pi\pi}^{\mathrm{r}} = \left[\frac{\partial^2 \gamma^{\mathrm{r}}}{\partial \pi^2}\right]_\tau$, $\gamma_\tau^{\mathrm{r}} = \left[\frac{\partial \gamma^{\mathrm{r}}}{\partial \tau}\right]_\pi$, $\gamma_{\tau\tau}^{\mathrm{r}} = \left[\frac{\partial^2 \gamma^{\mathrm{r}}}{\partial \tau^2}\right]_\pi$, $\gamma_{\pi\tau}^{\mathrm{r}} = \left[\frac{\partial^2 \gamma^{\mathrm{r}}}{\partial \pi \partial \tau}\right]$

Range of validity

Equation (15) covers region 2 of IAPWS-IF97 defined by the following range of temperature and pressure, see Fig. 1:

$$273.15\text{ K} \le T \le 623.15\text{ K} \qquad 0 < p \le p_s(T)_{\text{Eq.(30)}}$$
$$623.15\text{ K} < T \le 863.15\text{ K} \qquad 0 < p \le p(T)_{\text{Eq.(5)}}$$
$$863.15\text{ K} < T \le 1073.15\text{ K} \qquad 0 < p \le 100\text{ MPa}$$

In addition to the properties in the stable single-phase vapor region, Eq. (15) also yields reasonable values in the metastable-vapor region *for pressures above 10 MPa*. Equation (15) is not valid in the metastable-vapor region at pressures $p \le 10$ MPa; for this part of the metastable-vapor region see Section 6.2.

Note: For temperatures between 273.15 K and 273.16 K, the part of the range of validity between the pressures on the saturation-pressure line, Eq. (30), and on the sublimation line [10] corresponds to metastable states.

Computer-program verification

To assist the user in computer-program verification of Eq. (15), Table 15 contains test values of the most relevant properties.

Table 15. Thermodynamic property values calculated from Eq. (15) for selected values of T and p [a]

	T = 300 K, p = 0.0035 MPa	T = 700 K, p = 0.0035 MPa	T = 700 K, p = 30 MPa
$v/(\text{m}^3\ \text{kg}^{-1})$	$0.394\,913\,866 \times 10^{2}$	$0.923\,015\,898 \times 10^{2}$	$0.542\,946\,619 \times 10^{-2}$
$h/(\text{kJ kg}^{-1})$	$0.254\,991\,145 \times 10^{4}$	$0.333\,568\,375 \times 10^{4}$	$0.263\,149\,474 \times 10^{4}$
$u/(\text{kJ kg}^{-1})$	$0.241\,169\,160 \times 10^{4}$	$0.301\,262\,819 \times 10^{4}$	$0.246\,861\,076 \times 10^{4}$
$s/(\text{kJ kg}^{-1}\ \text{K}^{-1})$	$0.852\,238\,967 \times 10^{1}$	$0.101\,749\,996 \times 10^{2}$	$0.517\,540\,298 \times 10^{1}$
$c_p/(\text{kJ kg}^{-1}\ \text{K}^{-1})$	$0.191\,300\,162 \times 10^{1}$	$0.208\,141\,274 \times 10^{1}$	$0.103\,505\,092 \times 10^{2}$
$w/(\text{m s}^{-1})$	$0.427\,920\,172 \times 10^{3}$	$0.644\,289\,068 \times 10^{3}$	$0.480\,386\,523 \times 10^{3}$

[a] It is recommended to verify programmed functions using 8 byte real values for all three combinations of T and p given in this table.

6.2 Supplementary Equation for the Metastable-Vapor Region

As for the basic equation, Eq. (15), the supplementary equation for a part of the metastable-vapor region bounding region 2 is given in the dimensionless form of the specific Gibbs free energy, $\gamma = g/(RT)$, consisting of an ideal-gas part γ^{o} and a residual part γ^{r}, so that

$$\frac{g(p,T)}{RT} = \gamma(\pi,\tau) = \gamma^{\text{o}}(\pi,\tau) + \gamma^{\text{r}}(\pi,\tau) \ , \tag{18}$$

where $\pi = p/p^*$ and $\tau = T^*/T$ with R given by Eq. (1).

The equation for the ideal-gas part γ^{o} is identical with Eq. (16) except for the values of the two coefficients n_1^{o} and n_2^{o}, see Table 10. For the use of Eq. (16) as part of Eq. (18) the coefficients n_1^{o} and n_2^{o} were slightly readjusted to meet the high consistency requirement between Eqs. (18) and (15) regarding the properties h and s along the saturated vapor line; see below.

The equation for the residual part γ^{r} reads

$$\gamma^{\mathrm{r}} = \sum_{i=1}^{13} n_i\, \pi^{I_i} \left(\tau - 0.5\right)^{J_i} \quad , \tag{19}$$

where $\pi = p/p^*$ and $\tau = T^*/T$ with $p^* = 1$ MPa and $T^* = 540$ K. The coefficients n_i and exponents I_i and J_i of Eq. (19) are listed in Table 16.

Note: In the metastable-vapor region there are no experimental data to which an equation can be fitted. Thus, Eq. (18) is only based on input values extrapolated from the stable single-phase region 2. These extrapolations were performed with a special low-density gas equation [11] considered to be more suitable for such extrapolations into the metastable-vapor region than IAPWS-95 [3].

Table 16. Numerical values of the coefficients and exponents of the residual part γ^{r} of the dimensionless Gibbs free energy for the metastable-vapor region, Eq. (19)

i	I_i	J_i	n_i
1	1	0	$-0.733\,622\,601\,865\,06 \times 10^{-2}$
2	1	2	$-0.882\,238\,319\,431\,46 \times 10^{-1}$
3	1	5	$-0.723\,345\,552\,132\,45 \times 10^{-1}$
4	1	11	$-0.408\,131\,785\,344\,55 \times 10^{-2}$
5	2	1	$0.200\,978\,033\,802\,07 \times 10^{-2}$
6	2	7	$-0.530\,459\,218\,986\,42 \times 10^{-1}$
7	2	16	$-0.761\,904\,090\,869\,70 \times 10^{-2}$
8	3	4	$-0.634\,980\,376\,573\,13 \times 10^{-2}$
9	3	16	$-0.860\,430\,930\,285\,88 \times 10^{-1}$
10	4	7	$0.753\,215\,815\,227\,70 \times 10^{-2}$
11	4	10	$-0.792\,383\,754\,461\,39 \times 10^{-2}$
12	5	9	$-0.228\,881\,607\,784\,47 \times 10^{-3}$
13	5	10	$-0.264\,565\,014\,828\,10 \times 10^{-2}$

All thermodynamic properties can be derived from Eq. (18) by using the appropriate combinations of the ideal-gas part γ^{o}, Eq. (16), and the residual part γ^{r}, Eq. (19), of the dimensionless Gibbs free energy and their derivatives. Relations between the relevant thermodynamic properties and γ^{o} and γ^{r} and their derivatives are summarized in Table 12.

All required derivatives of the ideal-gas part and of the residual part of the dimensionless Gibbs free energy are explicitly given in Table 13 and Table 17, respectively.

Table 17. The residual part γ^{r} of the dimensionless Gibbs free energy and its derivatives [a] according to Eq. (19)

$$\gamma^{\mathrm{r}} = \sum_{i=1}^{13} n_i \, \pi^{I_i} \left(\tau - 0.5\right)^{J_i}$$

$$\gamma^{\mathrm{r}}_{\pi} = \sum_{i=1}^{13} n_i \, I_i \, \pi^{I_i - 1} \left(\tau - 0.5\right)^{J_i} \qquad \gamma^{\mathrm{r}}_{\pi\pi} = \sum_{i=1}^{13} n_i \, I_i \left(I_i - 1\right) \pi^{I_i - 2} \left(\tau - 0.5\right)^{J_i}$$

$$\gamma^{\mathrm{r}}_{\tau} = \sum_{i=1}^{13} n_i \, \pi^{I_i} J_i \left(\tau - 0.5\right)^{J_i - 1} \qquad \gamma^{\mathrm{r}}_{\tau\tau} = \sum_{i=1}^{13} n_i \, \pi^{I_i} J_i \left(J_i - 1\right)\left(\tau - 0.5\right)^{J_i - 2}$$

$$\gamma^{\mathrm{r}}_{\pi\tau} = \sum_{i=1}^{13} n_i \, I_i \, \pi^{I_i - 1} J_i \left(\tau - 0.5\right)^{J_i - 1}$$

[a] $\gamma^{\mathrm{r}}_{\pi} = \left[\frac{\partial \gamma^{\mathrm{r}}}{\partial \pi}\right]_{\tau}$, $\gamma^{\mathrm{r}}_{\pi\pi} = \left[\frac{\partial^2 \gamma^{\mathrm{r}}}{\partial \pi^2}\right]_{\tau}$, $\gamma^{\mathrm{r}}_{\tau} = \left[\frac{\partial \gamma^{\mathrm{r}}}{\partial \tau}\right]_{\pi}$, $\gamma^{\mathrm{r}}_{\tau\tau} = \left[\frac{\partial^2 \gamma^{\mathrm{r}}}{\partial \tau^2}\right]_{\pi}$, $\gamma^{\mathrm{r}}_{\pi\tau} = \left[\frac{\partial^2 \gamma^{\mathrm{r}}}{\partial \pi \partial \tau}\right]$

Range of validity

Equation (18) is valid in the metastable-vapor region from the saturated-vapor line to the 5 % equilibrium moisture line (determined from the equilibrium h' and h'' values calculated at the given pressure) for pressures from the triple-point pressure, see Eq. (9), up to 10 MPa.

Consistency with the basic equation

The consistency of Eq. (18) with the basic equation, Eq. (15), along the saturated vapor line is characterized by the following maximum inconsistencies regarding the properties v, h, c_p, s, g, and w:

$$
\begin{aligned}
|\Delta v|_{\max} &= 0.014\ \% & |\Delta s|_{\max} &= 0.082\ \mathrm{J\,kg^{-1}\,K^{-1}} \\
|\Delta h|_{\max} &= 0.043\ \mathrm{kJ\,kg^{-1}} & |\Delta g|_{\max} &= 0.023\ \mathrm{kJ\,kg^{-1}} \\
|\Delta c_p|_{\max} &= 0.78\ \% & |\Delta w|_{\max} &= 0.051\ \%\ .
\end{aligned}
$$

These maximum inconsistencies are clearly smaller than the consistency requirements on region boundaries corresponding to the so-called Prague values [13], which are given in Section 10.

Along the 10 MPa isobar in the metastable-vapor region, the transition between Eq. (18) and Eq. (15) is not smooth, which is however, not of importance for practical calculations.

Computer-program verification

To assist the user in computer-program verification of Eq. (18), Table 18 contains test values of the most relevant properties.

Table 18. Thermodynamic property values calculated from Eq. (18) for selected values of T and p [a]

	T = 450 K, p = 1 MPa	T = 440 K, p = 1 MPa	T = 450 K, p = 1.5 MPa
$v/(\mathrm{m^3\ kg^{-1}})$	0.192 516 540	0.186 212 297	0.121 685 206
$h/(\mathrm{kJ\ kg^{-1}})$	$0.276\ 881\ 115 \times 10^4$	$0.274\ 015\ 123 \times 10^4$	$0.272\ 134\ 539 \times 10^4$
$u/(\mathrm{kJ\ kg^{-1}})$	$0.257\ 629\ 461 \times 10^4$	$0.255\ 393\ 894 \times 10^4$	$0.253\ 881\ 758 \times 10^4$
$s/(\mathrm{kJ\ kg^{-1}\ K^{-1}})$	$0.656\ 660\ 377 \times 10^1$	$0.650\ 218\ 759 \times 10^1$	$0.629\ 170\ 440 \times 10^1$
$c_p/(\mathrm{kJ\ kg^{-1}\ K^{-1}})$	$0.276\ 349\ 265 \times 10^1$	$0.298\ 166\ 443 \times 10^1$	$0.362\ 795\ 578 \times 10^1$
$w/(\mathrm{m\ s^{-1}})$	$0.498\ 408\ 101 \times 10^3$	$0.489\ 363\ 295 \times 10^3$	$0.481\ 941\ 819 \times 10^3$

[a] It is recommended to verify programmed functions using 8 byte real values for all three combinations of T and p given in this table.

6.3 Backward Equations

For the calculation of properties as function of p, h or of p, s without any iteration, the two backward equations require extremely good numerical consistency with the basic equation. The exact requirements for these numerical consistencies were obtained from comprehensive test calculations for several characteristic power cycles. The result of these investigations, namely the assignment of the tolerable numerical inconsistencies between the basic equation, Eq. (15), and the corresponding backward equations, is given in Tables 23 and 28, respectively.

Region 2 is covered by *three* $T(p, h)$ and *three* $T(p, s)$ equations. Figure 2 shows the way in which region 2 is divided into three subregions for the backward equations. The boundary between the subregions 2a and 2b is the isobar p = 4 MPa; the boundary between the subregions 2b and 2c corresponds to the entropy line $s = 5.85\ \mathrm{kJ\ kg^{-1}\ K^{-1}}$.

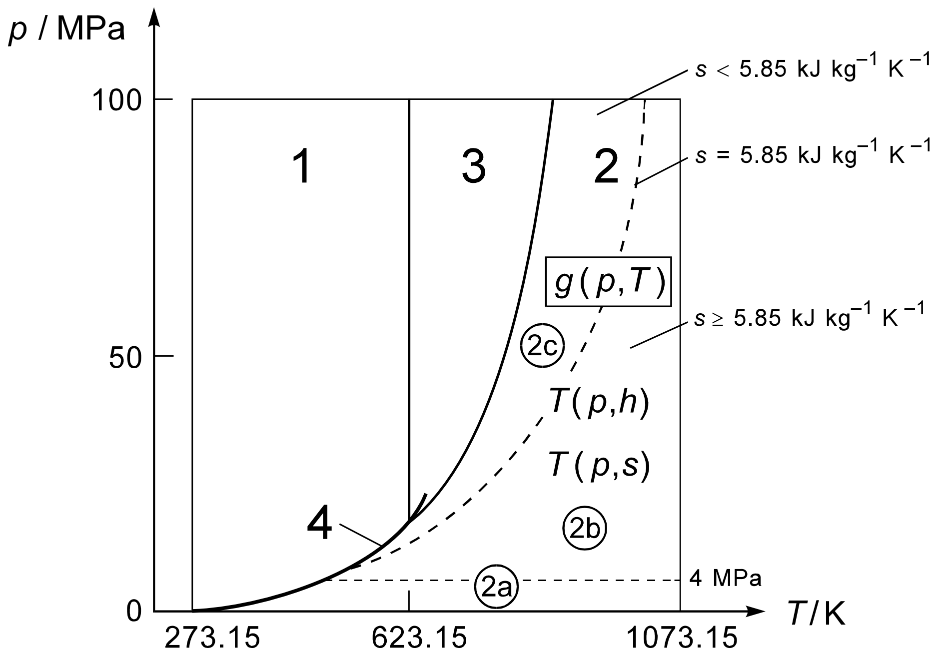

Fig. 2. Division of region 2 of IAPWS-IF97 into the three subregions 2a, 2b, and 2c for the backward equations $T(p,h)$ and $T(p,s)$.

In order to know whether the $T(p,h)$ equation for subregion 2b or for subregion 2c has to be used for given values of p and h, a special correlation equation for the boundary between subregions 2b and 2c (which approximates s = 5.85 kJ kg^{-1} K^{-1}) is needed; see Fig. 2. This boundary equation, called the B2bc-equation, is a simple quadratic pressure-enthalpy relation which reads

$$\pi = n_1 + n_2\eta + n_3\eta^2 \quad , \tag{20}$$

where $\pi = p/p^*$ and $\eta = h/h^*$ with $p^* = 1$ MPa and $h^* = 1$ kJ kg^{-1}. The coefficients n_1 to n_3 of Eq. (20) are listed in Table 19. Based on its simple form, Eq. (20) does not describe exactly the isentropic line s = 5.85 kJ kg^{-1} K^{-1}; the entropy values corresponding to this p-h relation are between s = 5.81 kJ kg^{-1} K^{-1} and s = 5.85 kJ kg^{-1} K^{-1}. The enthalpy-explicit form of Eq. (20) is as follows:

$$\eta = n_4 + \left[\left(\pi - n_5\right) / n_3\right]^{1/2} \quad , \tag{21}$$

with π and η according to Eq. (20) and the coefficients n_3 to n_5 listed in Table 19. Equations (20) and (21) give the boundary line between subregions 2b and 2c from the saturation state at T = 554.485 K and p_s = 6.546 70 MPa to T = 1019.32 K and p = 100 MPa.

For the backward equations $T(p,s)$ the boundary between subregions 2b and 2c is, based on the value s = 5.85 kJ kg^{-1} K^{-1} along this boundary, automatically defined for given values of p and s.

Table 19. Numerical values of the coefficients of the B2bc-equation, Eqs. (20) and (21), for defining the boundary between subregions 2b and 2c with respect to $T(p,h)$ calculations

i	n_i	i	n_i
1	$0.905\,842\,785\,147\,23 \times 10^{3}$	4	$0.265\,265\,719\,084\,28 \times 10^{4}$
2	$-0.679\,557\,863\,992\,41$	5	$0.452\,575\,789\,059\,48 \times 10^{1}$
3	$0.128\,090\,027\,301\,36 \times 10^{-3}$		

For *computer-program verification*, Eqs. (20) and (21) must meet the following *p-h* point: $p = 0.100\,000\,000 \times 10^{3}$ MPa , $h = 0.351\,600\,432\,3 \times 10^{4}$ kJ kg^{-1}.

6.3.1 The Backward Equations $T(p,h)$ for Subregions 2a, 2b, and 2c

The backward equation $T(p,h)$ for **subregion 2a** in its dimensionless form reads

$$\frac{T_{2\mathrm{a}}(p,h)}{T^*} = \theta_{2\mathrm{a}}(\pi,\eta) = \sum_{i=1}^{34} n_i\, \pi^{I_i} (\eta - 2.1)^{J_i} \,, \tag{22}$$

where $\theta = T/T^*$, $\pi = p/p^*$, and $\eta = h/h^*$ with $T^* = 1$ K, $p^* = 1$ MPa, and $h^* = 2000$ kJ kg^{-1}. The coefficients n_i and exponents I_i and J_i of Eq. (22) are listed in Table 20.

Table 20. Numerical values of the coefficients and exponents of the backward equation $T(p,h)$ for subregion 2a, Eq. (22)

i	I_i	J_i	n_i	i	I_i	J_i	n_i
1	0	0	$0.108\,989\,523\,182\,88 \times 10^{4}$	18	2	7	$0.116\,708\,730\,771\,07 \times 10^{2}$
2	0	1	$0.849\,516\,544\,955\,35 \times 10^{3}$	19	2	36	$0.128\,127\,984\,040\,46 \times 10^{9}$
3	0	2	$-0.107\,817\,480\,918\,26 \times 10^{3}$	20	2	38	$-0.985\,549\,096\,232\,76 \times 10^{9}$
4	0	3	$0.331\,536\,548\,012\,63 \times 10^{2}$	21	2	40	$0.282\,245\,469\,730\,02 \times 10^{10}$
5	0	7	$-0.742\,320\,167\,902\,48 \times 10^{1}$	22	2	42	$-0.359\,489\,714\,107\,03 \times 10^{10}$
6	0	20	$0.117\,650\,487\,243\,56 \times 10^{2}$	23	2	44	$0.172\,273\,499\,131\,97 \times 10^{10}$
7	1	0	$0.184\,457\,493\,557\,90 \times 10^{1}$	24	3	24	$-0.135\,513\,342\,407\,75 \times 10^{5}$
8	1	1	$-0.417\,927\,005\,496\,24 \times 10^{1}$	25	3	44	$0.128\,487\,346\,646\,50 \times 10^{8}$
9	1	2	$0.624\,781\,969\,358\,12 \times 10^{1}$	26	4	12	$0.138\,657\,242\,832\,26 \times 10^{1}$
10	1	3	$-0.173\,445\,631\,081\,14 \times 10^{2}$	27	4	32	$0.235\,988\,325\,565\,14 \times 10^{6}$
11	1	7	$-0.200\,581\,768\,620\,96 \times 10^{3}$	28	4	44	$-0.131\,052\,365\,450\,54 \times 10^{8}$
12	1	9	$0.271\,960\,654\,737\,96 \times 10^{3}$	29	5	32	$0.739\,998\,354\,747\,66 \times 10^{4}$
13	1	11	$-0.455\,113\,182\,858\,18 \times 10^{3}$	30	5	36	$-0.551\,966\,970\,300\,60 \times 10^{6}$
14	1	18	$0.309\,196\,886\,047\,55 \times 10^{4}$	31	5	42	$0.371\,540\,859\,962\,33 \times 10^{7}$
15	1	44	$0.252\,266\,403\,578\,72 \times 10^{6}$	32	6	34	$0.191\,277\,292\,396\,60 \times 10^{5}$
16	2	0	$-0.617\,074\,228\,683\,39 \times 10^{-2}$	33	6	44	$-0.415\,351\,648\,356\,34 \times 10^{6}$
17	2	2	$-0.310\,780\,466\,295\,83$	34	7	28	$-0.624\,598\,551\,925\,07 \times 10^{2}$

The backward equation $T(p,h)$ for **subregion 2b** in its dimensionless form reads

$$\frac{T_{2b}(p,h)}{T^*} = \theta_{2b}(\pi,\eta) = \sum_{i=1}^{38} n_i (\pi - 2)^{I_i} (\eta - 2.6)^{J_i} \quad , \tag{23}$$

where $\theta = T/T^*$, $\pi = p/p^*$, and $\eta = h/h^*$ with $T^* = 1$ K, $p^* = 1$ MPa, and $h^* = 2000$ kJ kg^{-1}. The coefficients n_i and exponents I_i and J_i of Eq. (23) are listed in Table 21.

Table 21. Numerical values of the coefficients and exponents of the backward equation $T(p,h)$ for subregion 2b, Eq. (23)

i	I_i	J_i	n_i	i	I_i	J_i	n_i
1	0	0	$0.148\,950\,410\,795\,16 \times 10^{4}$	20	2	40	$0.712\,803\,519\,595\,51 \times 10^{-4}$
2	0	1	$0.743\,077\,983\,140\,34 \times 10^{3}$	21	3	1	$0.110\,328\,317\,899\,99 \times 10^{-3}$
3	0	2	$-0.977\,083\,187\,978\,37 \times 10^{2}$	22	3	2	$0.189\,552\,483\,879\,02 \times 10^{-3}$
4	0	12	$0.247\,424\,647\,056\,74 \times 10^{1}$	23	3	12	$0.308\,915\,411\,605\,37 \times 10^{-2}$
5	0	18	$-0.632\,813\,200\,160\,26$	24	3	24	$0.135\,555\,045\,549\,49 \times 10^{-2}$
6	0	24	$0.113\,859\,521\,296\,58 \times 10^{1}$	25	4	2	$0.286\,402\,374\,774\,56 \times 10^{-6}$
7	0	28	$-0.478\,118\,636\,486\,25$	26	4	12	$-0.107\,798\,573\,575\,12 \times 10^{-4}$
8	0	40	$0.852\,081\,234\,315\,44 \times 10^{-2}$	27	4	18	$-0.764\,627\,124\,548\,14 \times 10^{-4}$
9	1	0	$0.937\,471\,473\,779\,32$	28	4	24	$0.140\,523\,928\,183\,16 \times 10^{-4}$
10	1	2	$0.335\,931\,186\,049\,16 \times 10^{1}$	29	4	28	$-0.310\,838\,143\,314\,34 \times 10^{-4}$
11	1	6	$0.338\,093\,556\,014\,54 \times 10^{1}$	30	4	40	$-0.103\,027\,382\,121\,03 \times 10^{-5}$
12	1	12	$0.168\,445\,396\,719\,04$	31	5	18	$0.282\,172\,816\,350\,40 \times 10^{-6}$
13	1	18	$0.738\,757\,452\,366\,95$	32	5	24	$0.127\,049\,022\,719\,45 \times 10^{-5}$
14	1	24	$-0.471\,287\,374\,361\,86$	33	5	40	$0.738\,033\,534\,682\,92 \times 10^{-7}$
15	1	28	$0.150\,202\,731\,397\,07$	34	6	28	$-0.110\,301\,392\,389\,09 \times 10^{-7}$
16	1	40	$-0.217\,641\,142\,197\,50 \times 10^{-2}$	35	7	2	$-0.814\,563\,652\,078\,33 \times 10^{-13}$
17	2	2	$-0.218\,107\,553\,247\,61 \times 10^{-1}$	36	7	28	$-0.251\,805\,456\,829\,62 \times 10^{-10}$
18	2	8	$-0.108\,297\,844\,036\,77$	37	9	1	$-0.175\,652\,339\,694\,07 \times 10^{-17}$
19	2	18	$-0.463\,333\,246\,358\,12 \times 10^{-1}$	38	9	40	$0.869\,341\,563\,441\,63 \times 10^{-14}$

The backward equation $T(p,h)$ for **subregion 2c** in its dimensionless form reads

$$\frac{T_{2c}(p,h)}{T^*} = \theta_{2c}(\pi,\eta) = \sum_{i=1}^{23} n_i (\pi + 25)^{I_i} (\eta - 1.8)^{J_i} \quad , \tag{24}$$

where $\theta = T/T^*$, $\pi = p/p^*$, and $\eta = h/h^*$ with $T^* = 1$ K, $p^* = 1$ MPa, and $h^* = 2000$ kJ kg^{-1}. The coefficients n_i and exponents I_i and J_i of Eq. (24) are listed in Table 22.

Table 22. Numerical values of the coefficients and exponents of the backward equation $T(p,h)$ for subregion 2c, Eq. (24)

i	I_i	J_i	n_i
1	−7	0	$-0.323\,683\,985\,552\,42 \times 10^{13}$
2	−7	4	$0.732\,633\,509\,021\,81 \times 10^{13}$
3	−6	0	$0.358\,250\,899\,454\,47 \times 10^{12}$
4	−6	2	$-0.583\,401\,318\,515\,90 \times 10^{12}$
5	−5	0	$-0.107\,830\,682\,174\,70 \times 10^{11}$
6	−5	2	$0.208\,255\,445\,631\,71 \times 10^{11}$
7	−2	0	$0.610\,747\,835\,645\,16 \times 10^{6}$
8	−2	1	$0.859\,777\,225\,355\,80 \times 10^{6}$
9	−1	0	$-0.257\,457\,236\,041\,70 \times 10^{5}$
10	−1	2	$0.310\,810\,884\,227\,14 \times 10^{5}$
11	0	0	$0.120\,823\,158\,659\,36 \times 10^{4}$
12	0	1	$0.482\,197\,551\,092\,55 \times 10^{3}$
13	1	4	$0.379\,660\,012\,724\,86 \times 10^{1}$
14	1	8	$-0.108\,429\,848\,800\,77 \times 10^{2}$
15	2	4	$-0.453\,641\,726\,766\,60 \times 10^{-1}$
16	6	0	$0.145\,591\,156\,586\,98 \times 10^{-12}$
17	6	1	$0.112\,615\,974\,072\,30 \times 10^{-11}$
18	6	4	$-0.178\,049\,822\,406\,86 \times 10^{-10}$
19	6	10	$0.123\,245\,796\,908\,32 \times 10^{-6}$
20	6	12	$-0.116\,069\,211\,309\,84 \times 10^{-5}$
21	6	16	$0.278\,463\,670\,885\,54 \times 10^{-4}$
22	6	20	$-0.592\,700\,384\,741\,76 \times 10^{-3}$
23	6	22	$0.129\,185\,829\,918\,78 \times 10^{-2}$

Range of validity

Equations (22), (23), and (24) are only valid in the respective subregion 2a, 2b, and 2c which do not include the metastable-vapor region. The boundaries between these subregions are defined at the beginning of Section 6.3; the lowest pressure for which Eq. (22) is valid amounts to 611.2127 Pa corresponding to the saturation pressure at 273.15 K calculated from Eq. (30).

Numerical consistency with the basic equation

For ten million random pairs of p and h covering each of the subregions 2a, 2b, and 2c, the differences ΔT between temperatures calculated from Eqs. (22) to (24), respectively, and from Eq. (15) were determined. The corresponding maximum and root-mean-square differences are listed in Table 23 together with the tolerated differences according to the numerical consistency requirements with respect to Eq. (15).

Table 23. Maximum differences $|\Delta T|_{\max}$ and root-mean-square differences ΔT_{RMS} between temperatures calculated from Eqs. (22) to (24), and from Eq. (15) in comparison with the tolerated differences $|\Delta T|_{\mathrm{tol}}$

Subregion	Equation	$\lvert\Delta T\rvert_{\mathrm{tol}}$ /mK	$\lvert\Delta T\rvert_{\max}$ /mK	ΔT_{RMS} /mK
2a	22	10	9.3	2.9
2b	23	10	9.6	3.9
2c	24	25	23.7	10.4

Computer-program verification

To assist the user in computer-program verification of Eqs. (22) to (24), Table 24 contains the corresponding test values.

Table 24. Temperature values calculated from Eqs. (22) to (24) for selected values of p and h [a]

Equation	p/MPa	h/(kJ kg^{-1})	T/K
	0.001	3000	$0.534\,433\,241 \times 10^{3}$
22	3	3000	$0.575\,373\,370 \times 10^{3}$
	3	4000	$0.101\,077\,577 \times 10^{4}$
	5	3500	$0.801\,299\,102 \times 10^{3}$
23	5	4000	$0.101\,531\,583 \times 10^{4}$
	25	3500	$0.875\,279\,054 \times 10^{3}$
	40	2700	$0.743\,056\,411 \times 10^{3}$
24	60	2700	$0.791\,137\,067 \times 10^{3}$
	60	3200	$0.882\,756\,860 \times 10^{3}$

[a] It is recommended to verify the programmed equations using 8 byte real values for all three combinations of p and h given in this table for each of the equations.

6.3.2 The Backward Equations $T(p,s)$ for Subregions 2a, 2b, and 2c

The backward equation $T(p,s)$ for **subregion 2a** in its dimensionless form reads

$$\frac{T_{2\mathrm{a}}(p,s)}{T^*} = \theta_{2\mathrm{a}}(\pi,\sigma) = \sum_{i=1}^{46} n_i\, \pi^{I_i} (\sigma-2)^{J_i} \quad , \tag{25}$$

where $\theta = T/T^*$, $\pi = p/p^*$, and $\sigma = s/s^*$ with $T^* = 1$ K, $p^* = 1$ MPa, and $s^* = 2$ kJ kg^{-1} K^{-1}. The coefficients n_i and exponents I_i and J_i of Eq. (25) are listed in Table 25.

Table 25. Numerical values of the coefficients and exponents of the backward equation $T(p,s)$ for subregion 2a, Eq. (25)

i	I_i	J_i	n_i	i	I_i	J_i	n_i
1	−1.5	−24	$-0.392\,359\,838\,619\,84 \times 10^{6}$	24	−0.25	−11	$-0.597\,806\,388\,727\,18 \times 10^{4}$
2	−1.5	−23	$0.515\,265\,738\,272\,70 \times 10^{6}$	25	−0.25	−6	$-0.704\,014\,639\,268\,62 \times 10^{3}$
3	−1.5	−19	$0.404\,824\,431\,610\,48 \times 10^{5}$	26	0.25	1	$0.338\,367\,841\,075\,53 \times 10^{3}$
4	−1.5	−13	$-0.321\,937\,909\,239\,02 \times 10^{3}$	27	0.25	4	$0.208\,627\,866\,351\,87 \times 10^{2}$
5	−1.5	−11	$0.969\,614\,242\,186\,94 \times 10^{2}$	28	0.25	8	$0.338\,341\,726\,561\,96 \times 10^{-1}$
6	−1.5	−10	$-0.228\,678\,463\,717\,73 \times 10^{2}$	29	0.25	11	$-0.431\,244\,284\,148\,93 \times 10^{-4}$
7	−1.25	−19	$-0.449\,429\,141\,243\,57 \times 10^{6}$	30	0.5	0	$0.166\,537\,913\,564\,12 \times 10^{3}$
8	−1.25	−15	$-0.501\,183\,360\,201\,66 \times 10^{4}$	31	0.5	1	$-0.139\,862\,920\,558\,98 \times 10^{3}$
9	−1.25	−6	$0.356\,844\,635\,600\,15$	32	0.5	5	$-0.788\,495\,479\,998\,72$
10	−1.0	−26	$0.442\,353\,358\,481\,90 \times 10^{5}$	33	0.5	6	$0.721\,324\,117\,538\,72 \times 10^{-1}$
11	−1.0	−21	$-0.136\,733\,888\,117\,08 \times 10^{5}$	34	0.5	10	$-0.597\,548\,393\,982\,83 \times 10^{-2}$
12	−1.0	−17	$0.421\,632\,602\,078\,64 \times 10^{6}$	35	0.5	14	$-0.121\,413\,589\,539\,04 \times 10^{-4}$
13	−1.0	−16	$0.225\,169\,258\,374\,75 \times 10^{5}$	36	0.5	16	$0.232\,270\,967\,338\,71 \times 10^{-6}$
14	−1.0	−9	$0.474\,421\,448\,656\,46 \times 10^{3}$	37	0.75	0	$-0.105\,384\,635\,661\,94 \times 10^{2}$
15	−1.0	−8	$-0.149\,311\,307\,976\,47 \times 10^{3}$	38	0.75	4	$0.207\,189\,254\,965\,02 \times 10^{1}$
16	−0.75	−15	$-0.197\,811\,263\,204\,52 \times 10^{6}$	39	0.75	9	$-0.721\,931\,552\,604\,27 \times 10^{-1}$
17	−0.75	−14	$-0.235\,543\,994\,707\,60 \times 10^{5}$	40	0.75	17	$0.207\,498\,870\,811\,20 \times 10^{-6}$
18	−0.5	−26	$-0.190\,706\,163\,020\,76 \times 10^{5}$	41	1.0	7	$-0.183\,406\,579\,113\,79 \times 10^{-1}$
19	−0.5	−13	$0.553\,756\,698\,831\,64 \times 10^{5}$	42	1.0	18	$0.290\,362\,723\,486\,96 \times 10^{-6}$
20	−0.5	−9	$0.382\,936\,914\,373\,63 \times 10^{4}$	43	1.25	3	$0.210\,375\,278\,936\,19$
21	−0.5	−7	$-0.603\,918\,605\,805\,67 \times 10^{3}$	44	1.25	15	$0.256\,812\,397\,299\,99 \times 10^{-3}$
22	−0.25	−27	$0.193\,631\,026\,203\,31 \times 10^{4}$	45	1.5	5	$-0.127\,990\,029\,337\,81 \times 10^{-1}$
23	−0.25	−25	$0.426\,606\,436\,986\,10 \times 10^{4}$	46	1.5	18	$-0.821\,981\,026\,520\,18 \times 10^{-5}$

The backward equation $T(p,s)$ for **subregion 2b** in its dimensionless form reads

$$\frac{T_{2\mathrm{b}}(p,s)}{T^*} = \theta_{2\mathrm{b}}(\pi,\sigma) = \sum_{i=1}^{44} n_i\, \pi^{I_i} (10-\sigma)^{J_i} \quad , \tag{26}$$

where $\theta = T/T^*$, $\pi = p/p^*$, and $\sigma = s/s^*$ with $T^* = 1\ \mathrm{K}$, $p^* = 1\ \mathrm{MPa}$, and $s^* = 0.7853\ \mathrm{kJ\ kg^{-1}\,K^{-1}}$. The coefficients n_i and exponents I_i and J_i of Eq. (26) are listed in Table 26.

Table 26. Numerical values of the coefficients and exponents of the backward equation $T(p,s)$ for subregion 2b, Eq. (26)

i	I_i	J_i	n_i	i	I_i	J_i	n_i
1	−6	0	$0.316\,876\,650\,834\,97 \times 10^{6}$	23	0	2	$0.417\,273\,471\,596\,10 \times 10^{2}$
2	−6	11	$0.208\,641\,758\,818\,58 \times 10^{2}$	24	0	4	$0.219\,325\,494\,345\,32 \times 10^{1}$
3	−5	0	$-0.398\,593\,998\,035\,99 \times 10^{6}$	25	0	5	$-0.103\,200\,500\,090\,77 \times 10^{1}$
4	−5	11	$-0.218\,160\,585\,188\,77 \times 10^{2}$	26	0	6	$0.358\,829\,435\,167\,03$
5	−4	0	$0.223\,697\,851\,942\,42 \times 10^{6}$	27	0	9	$0.525\,114\,537\,260\,66 \times 10^{-2}$
6	−4	1	$-0.278\,417\,034\,458\,17 \times 10^{4}$	28	1	0	$0.128\,389\,164\,507\,05 \times 10^{2}$
7	−4	11	$0.992\,074\,360\,714\,80 \times 10^{1}$	29	1	1	$-0.286\,424\,372\,193\,81 \times 10^{1}$
8	−3	0	$-0.751\,975\,122\,991\,57 \times 10^{5}$	30	1	2	$0.569\,126\,836\,648\,55$
9	−3	1	$0.297\,086\,059\,511\,58 \times 10^{4}$	31	1	3	$-0.999\,629\,545\,849\,31 \times 10^{-1}$
10	−3	11	$-0.344\,068\,785\,485\,26 \times 10^{1}$	32	1	7	$-0.326\,320\,377\,784\,59 \times 10^{-2}$
11	−3	12	$0.388\,155\,642\,491\,15$	33	1	8	$0.233\,209\,225\,767\,23 \times 10^{-3}$
12	−2	0	$0.175\,112\,950\,857\,50 \times 10^{5}$	34	2	0	$-0.153\,348\,098\,574\,50$
13	−2	1	$-0.142\,371\,128\,544\,49 \times 10^{4}$	35	2	1	$0.290\,722\,882\,399\,02 \times 10^{-1}$
14	−2	6	$0.109\,438\,033\,641\,67 \times 10^{1}$	36	2	5	$0.375\,347\,027\,411\,67 \times 10^{-3}$
15	−2	10	$0.899\,716\,193\,084\,95$	37	3	0	$0.172\,966\,917\,024\,11 \times 10^{-2}$
16	−1	0	$-0.337\,597\,400\,989\,58 \times 10^{4}$	38	3	1	$-0.385\,560\,508\,445\,04 \times 10^{-3}$
17	−1	1	$0.471\,628\,858\,183\,55 \times 10^{3}$	39	3	3	$-0.350\,177\,122\,926\,08 \times 10^{-4}$
18	−1	5	$-0.191\,882\,419\,936\,79 \times 10^{1}$	40	4	0	$-0.145\,663\,936\,314\,92 \times 10^{-4}$
19	−1	8	$0.410\,785\,804\,921\,96$	41	4	1	$0.564\,208\,572\,672\,69 \times 10^{-5}$
20	−1	9	$-0.334\,653\,781\,720\,97$	42	5	0	$0.412\,861\,500\,746\,05 \times 10^{-7}$
21	0	0	$0.138\,700\,347\,775\,05 \times 10^{4}$	43	5	1	$-0.206\,846\,711\,188\,24 \times 10^{-7}$
22	0	1	$-0.406\,633\,261\,958\,38 \times 10^{3}$	44	5	2	$0.164\,093\,936\,747\,25 \times 10^{-8}$

The backward equation $T(p,s)$ for **subregion 2c** in its dimensionless form reads

$$\frac{T_{2c}(p,s)}{T^*} = \theta_{2c}(\pi,\sigma) = \sum_{i=1}^{30} n_i\, \pi^{I_i} (2-\sigma)^{J_i} \ , \tag{27}$$

where $\theta = T/T^*$, $\pi = p/p^*$, and $\sigma = s/s^*$ with $T^* = 1$ K, $p^* = 1$ MPa, and $s^* = 2.9251$ kJ kg^{-1} K^{-1}. The coefficients n_i and exponents I_i and J_i of Eq. (27) are listed in Table 27.

Table 27. Numerical values of the coefficient s and exponents of the backward equation $T(p,s)$ for subregion 2c, Eq. (27)

i	I_i	J_i	n_i	i	I_i	J_i	n_i
1	−2	0	$0.909\,685\,010\,053\,65 \times 10^{3}$	16	3	1	$-0.145\,970\,082\,847\,53 \times 10^{-1}$
2	−2	1	$0.240\,456\,670\,884\,20 \times 10^{4}$	17	3	5	$0.566\,311\,756\,310\,27 \times 10^{-2}$
3	−1	0	$-0.591\,623\,263\,871\,30 \times 10^{3}$	18	4	0	$-0.761\,558\,645\,845\,77 \times 10^{-4}$
4	0	0	$0.541\,454\,041\,280\,74 \times 10^{3}$	19	4	1	$0.224\,403\,429\,193\,32 \times 10^{-3}$
5	0	1	$-0.270\,983\,084\,111\,92 \times 10^{3}$	20	4	4	$-0.125\,610\,950\,134\,13 \times 10^{-4}$
6	0	2	$0.979\,765\,250\,979\,26 \times 10^{3}$	21	5	0	$0.633\,231\,326\,609\,34 \times 10^{-6}$
7	0	3	$-0.469\,667\,729\,594\,35 \times 10^{3}$	22	5	1	$-0.205\,419\,896\,753\,75 \times 10^{-5}$
8	1	0	$0.143\,992\,746\,047\,23 \times 10^{2}$	23	5	2	$0.364\,053\,703\,900\,82 \times 10^{-7}$
9	1	1	$-0.191\,042\,042\,304\,29 \times 10^{2}$	24	6	0	$-0.297\,598\,977\,892\,15 \times 10^{-8}$
10	1	3	$0.532\,991\,671\,119\,71 \times 10^{1}$	25	6	1	$0.101\,366\,185\,297\,63 \times 10^{-7}$
11	1	4	$-0.212\,529\,753\,759\,34 \times 10^{2}$	26	7	0	$0.599\,257\,196\,923\,51 \times 10^{-11}$
12	2	0	$-0.311\,473\,344\,137\,60$	27	7	1	$-0.206\,778\,701\,051\,64 \times 10^{-10}$
13	2	1	$0.603\,348\,408\,946\,23$	28	7	3	$-0.208\,742\,781\,818\,86 \times 10^{-10}$
14	2	2	$-0.427\,648\,397\,025\,09 \times 10^{-1}$	29	7	4	$0.101\,621\,668\,250\,89 \times 10^{-9}$
15	3	0	$0.581\,855\,972\,552\,59 \times 10^{-2}$	30	7	5	$-0.164\,298\,282\,813\,47 \times 10^{-9}$

Range of validity

Equations (25), (26), and (27) are only valid in the respective subregion 2a, 2b, and 2c which do not include the metastable-vapor region. The boundaries between these subregions are defined at the beginning of Section 6.3; the lowest pressure for which Eq. (25) is valid amounts to 611.153 Pa corresponding to the sublimation pressure [10] at 273.15 K.

Numerical consistency with the basic equation

For ten million random pairs of p and s covering each of the subregions 2a, 2b, and 2c, the differences ΔT between temperatures calculated from Eqs. (25) to (27), respectively, and from Eq. (15) were determined. The corresponding maximum and root-mean-square differences are listed in Table 28 together with the tolerated differences according to the numerical consistency requirements with respect to Eq. (15).

Table 28. Maximum differences $|\Delta T|_{max}$ and root-mean-square differences ΔT_{RMS} between temperatures calculated from Eqs. (25) to (27), and from Eq. (15) in comparison with the tolerated differences $|\Delta T|_{tol}$

Subregion	Equation	$\|\Delta T\|_{tol}$ /mK	$\|\Delta T\|_{max}$ /mK	ΔT_{RMS} /mK
2a	25	10	8.8	1.2
2b	26	10	6.5	2.8
2c	27	25	19.0	8.3

Computer-program verification

To assist the user in computer-program verification of Eqs. (25) to (27), Table 29 contains the corresponding test values.

Table 29. Temperature values calculated from Eqs. (25) to (27) for selected values of p and s [a]

Equation	p/MPa	s/(kJ kg^{-1} K^{-1})	T/K
25	0.1	7.5	$0.399\,517\,097 \times 10^{3}$
	0.1	8	$0.514\,127\,081 \times 10^{3}$
	2.5	8	$0.103\,984\,917 \times 10^{4}$
26	8	6	$0.600\,484\,040 \times 10^{3}$
	8	7.5	$0.106\,495\,556 \times 10^{4}$
	90	6	$0.103\,801\,126 \times 10^{4}$
27	20	5.75	$0.697\,992\,849 \times 10^{3}$
	80	5.25	$0.854\,011\,484 \times 10^{3}$
	80	5.75	$0.949\,017\,998 \times 10^{3}$

[a] It is recommended to verify the programmed equations using 8 byte real values for all three combinations of p and s given in this table for each of the equations.

7 Basic Equation for Region 3

This section contains all details relevant for the use of the basic equation of region 3 of IAPWS-IF97. Information about the consistency of the basic equation of this region with the basic equations of regions 1, 2, and 4 along the corresponding region boundaries is summarized in Section 10. The auxiliary equation for defining the boundary between regions 2 and 3 is given in Section 4. Section 11 contains the results of computing-time comparisons between IAPWS-IF97 and IFC-67. The estimates of uncertainty of the most relevant properties can be found in Section 12.

The basic equation for this region is a fundamental equation for the specific Helmholtz free energy f. This equation is expressed in dimensionless form, $\phi = f\,/\,(RT)$, and reads

$$\frac{f(\rho,T)}{RT} = \phi(\delta,\tau) = n_1 \ln\delta + \sum_{i=2}^{40} n_i\,\delta^{I_i}\tau^{J_i}\,, \tag{28}$$

where $\delta = \rho/\rho^*$, $\tau = T^*/T$ with $\rho^* = \rho_c$, $T^* = T_c$ and R, T_c, and ρ_c given by Eqs. (1), (2), and (4). The coefficients n_i and exponents I_i and J_i of Eq. (28) are listed in Table 30.

In addition to representing the thermodynamic properties in the single-phase region, Eq. (28) meets the phase-equilibrium condition (equality of specific Gibbs free energy for coexisting vapor + liquid states; see Table 31) along the saturation line for $T \geq 623.15$ K to T_c. Moreover, Eq. (28) reproduces exactly the critical parameters according to Eqs. (2) to (4) and yields zero for the first two pressure derivatives with respect to density at the critical point.

Table 30. Numerical values of the coefficients and exponents of the dimensionless Helmholtz free energy for region 3, Eq. (28)

i	I_i	J_i	n_i	i	I_i	J_i	n_i
1	–	–	$0.106\,580\,700\,285\,13 \times 10^{1}$	21	3	4	$-0.201\,899\,150\,235\,70 \times 10^{1}$
2	0	0	$-0.157\,328\,452\,902\,39 \times 10^{2}$	22	3	16	$-0.821\,476\,371\,739\,63 \times 10^{-2}$
3	0	1	$0.209\,443\,969\,743\,07 \times 10^{2}$	23	3	26	$-0.475\,960\,357\,349\,23$
4	0	2	$-0.768\,677\,078\,787\,16 \times 10^{1}$	24	4	0	$0.439\,840\,744\,735\,00 \times 10^{-1}$
5	0	7	$0.261\,859\,477\,879\,54 \times 10^{1}$	25	4	2	$-0.444\,764\,354\,287\,39$
6	0	10	$-0.280\,807\,811\,486\,20 \times 10^{1}$	26	4	4	$0.905\,720\,707\,197\,33$
7	0	12	$0.120\,533\,696\,965\,17 \times 10^{1}$	27	4	26	$0.705\,224\,500\,879\,67$
8	0	23	$-0.845\,668\,128\,125\,02 \times 10^{-2}$	28	5	1	$0.107\,705\,126\,263\,32$
9	1	2	$-0.126\,543\,154\,777\,14 \times 10^{1}$	29	5	3	$-0.329\,136\,232\,589\,54$
10	1	6	$-0.115\,244\,078\,066\,81 \times 10^{1}$	30	5	26	$-0.508\,710\,620\,411\,58$
11	1	15	$0.885\,210\,439\,843\,18$	31	6	0	$-0.221\,754\,008\,730\,96 \times 10^{-1}$
12	1	17	$-0.642\,077\,651\,816\,07$	32	6	2	$0.942\,607\,516\,650\,92 \times 10^{-1}$
13	2	0	$0.384\,934\,601\,866\,71$	33	6	26	$0.164\,362\,784\,479\,61$
14	2	2	$-0.852\,147\,088\,242\,06$	34	7	2	$-0.135\,033\,722\,413\,48 \times 10^{-1}$
15	2	6	$0.489\,722\,815\,418\,77 \times 10^{1}$	35	8	26	$-0.148\,343\,453\,524\,72 \times 10^{-1}$
16	2	7	$-0.305\,026\,172\,569\,65 \times 10^{1}$	36	9	2	$0.579\,229\,536\,280\,84 \times 10^{-3}$
17	2	22	$0.394\,205\,368\,791\,54 \times 10^{-1}$	37	9	26	$0.323\,089\,047\,037\,11 \times 10^{-2}$
18	2	26	$0.125\,584\,084\,243\,08$	38	10	0	$0.809\,648\,029\,962\,15 \times 10^{-4}$
19	3	0	$-0.279\,993\,296\,987\,10$	39	10	1	$-0.165\,576\,797\,950\,37 \times 10^{-3}$
20	3	2	$0.138\,997\,995\,694\,60 \times 10^{1}$	40	11	26	$-0.449\,238\,990\,618\,15 \times 10^{-4}$

All thermodynamic properties can be derived from Eq. (28) by using the appropriate combinations of the dimensionless Helmholtz free energy and its derivatives. Relations between the relevant thermodynamic properties and ϕ and its derivatives are summarized in Table 31. All required derivatives of the dimensionless Helmholtz free energy are explicitly given in Table 32.

Table 31. Relations of thermodynamic properties to the dimensionless Helmholtz free energy ϕ and its derivatives[a] when using Eq. (28)

Property	Relation
Pressure $p = \rho^2 (\partial f/\partial \rho)_T$	$\dfrac{p(\delta,\tau)}{\rho RT} = \delta\phi_\delta$
Specific internal energy $u = f - T(\partial f/\partial T)_\rho$	$\dfrac{u(\delta,\tau)}{RT} = \tau\phi_\tau$
Specific entropy $s = -(\partial f/\partial T)_\rho$	$\dfrac{s(\delta,\tau)}{R} = \tau\phi_\tau - \phi$
Specific enthalpy $h = f - T(\partial f/\partial T)_\rho + \rho(\partial f/\partial \rho)_T$	$\dfrac{h(\delta,\tau)}{RT} = \tau\phi_\tau + \delta\phi_\delta$
Specific isochoric heat capacity $c_v = (\partial u/\partial T)_\rho$	$\dfrac{c_v(\delta,\tau)}{R} = -\tau^2\phi_{\tau\tau}$
Specific isobaric heat capacity $c_p = (\partial h/\partial T)_p$	$\dfrac{c_p(\delta,\tau)}{R} = -\tau^2\phi_{\tau\tau} + \dfrac{(\delta\phi_\delta - \delta\tau\phi_{\delta\tau})^2}{2\delta\phi_\delta + \delta^2\phi_{\delta\delta}}$
Speed of sound $w = (\partial p/\partial \rho)_s^{1/2}$	$\dfrac{w^2(\delta,\tau)}{RT} = 2\delta\phi_\delta + \delta^2\phi_{\delta\delta} - \dfrac{(\delta\phi_\delta - \delta\tau\phi_{\delta\tau})^2}{\tau^2\phi_{\tau\tau}}$
Phase-equilibrium condition (Maxwell criterion)	$\dfrac{p_\mathrm{s}}{RT\rho'} = \delta'\phi_\delta(\delta',\tau)$; $\dfrac{p_\mathrm{s}}{RT\rho''} = \delta''\phi_\delta(\delta'',\tau)$ $\dfrac{p_\mathrm{s}}{RT}\left(\dfrac{1}{\rho''} - \dfrac{1}{\rho'}\right) = \phi(\delta',\tau) - \phi(\delta'',\tau)$

[a] $\phi_\delta = \left[\dfrac{\partial \phi}{\partial \delta}\right]_\tau$, $\phi_{\delta\delta} = \left[\dfrac{\partial^2 \phi}{\partial \delta^2}\right]_\tau$, $\phi_\tau = \left[\dfrac{\partial \phi}{\partial \tau}\right]_\delta$, $\phi_{\tau\tau} = \left[\dfrac{\partial^2 \phi}{\partial \tau^2}\right]_\delta$, $\phi_{\delta\tau} = \left[\dfrac{\partial^2 \phi}{\partial \delta \partial \tau}\right]$

Table 32. The dimensionless Helmholtz free energy equation and its derivatives[a] according to Eq. (28)

$$\phi = n_1 \ln \delta + \sum_{i=2}^{40} n_i \ \delta^{I_i} \ \tau^{J_i}$$

$$\phi_\delta = n_1 / \delta + \sum_{i=2}^{40} n_i \ I_i \, \delta^{I_i - 1} \ \tau^{J_i} \qquad \phi_{\delta\delta} = -n_1 / \delta^2 + \sum_{i=2}^{40} n_i \ I_i \left(I_i - 1\right) \delta^{I_i - 2} \ \tau^{J_i}$$

$$\phi_\tau = 0 + \sum_{i=2}^{40} n_i \ \delta^{I_i} \ J_i \, \tau^{J_i - 1} \qquad \phi_{\tau\tau} = 0 + \sum_{i=2}^{40} n_i \ \delta^{I_i} \ J_i \left(J_i - 1\right) \tau^{J_i - 2}$$

$$\phi_{\delta\tau} = 0 + \sum_{i=2}^{40} n_i \ I_i \, \delta^{I_i - 1} \ J_i \, \tau^{J_i - 1}$$

[a] $\phi_\delta = \left[\frac{\partial \phi}{\partial \delta}\right]_\tau, \ \phi_{\delta\delta} = \left[\frac{\partial^2 \phi}{\partial \delta^2}\right]_\tau, \ \phi_\tau = \left[\frac{\partial \phi}{\partial \tau}\right]_\delta, \ \phi_{\tau\tau} = \left[\frac{\partial^2 \phi}{\partial \tau^2}\right]_\delta, \ \phi_{\delta\tau} = \left[\frac{\partial^2 \phi}{\partial \delta \partial \tau}\right]$

Range of validity

Equation (28) covers region 3 of IAPWS-IF97 defined by the following range of temperature and pressure, see Fig. 1:

$$623.15 \text{ K} \le T \le T(p)_{\text{Eq.(6)}} \qquad p(T)_{\text{Eq.(5)}} \le p \le 100 \text{ MPa} .$$

In addition to the properties in the stable single-phase region defined above, Eq. (28) also yields reasonable values in the metastable regions (superheated liquid and subcooled steam) close to the saturated liquid and saturated vapor line.

Computer-program verification

To assist the user in computer-program verification of Eq. (28), Table 33 contains test values of the most relevant properties.

Table 33. Thermodynamic property values calculated from Eq. (28) for selected values of T and ρ[a]

	T = 650 K, ρ = 500 kg m^{-3}	T = 650 K, ρ = 200 kg m^{-3}	T = 750 K, ρ = 500 kg m^{-3}
p/MPa	$0.255\,837\,018 \times 10^{2}$	$0.222\,930\,643 \times 10^{2}$	$0.783\,095\,639 \times 10^{2}$
h/(kJ kg^{-1})	$0.186\,343\,019 \times 10^{4}$	$0.237\,512\,401 \times 10^{4}$	$0.225\,868\,845 \times 10^{4}$
u/(kJ kg^{-1})	$0.181\,226\,279 \times 10^{4}$	$0.226\,365\,868 \times 10^{4}$	$0.210\,206\,932 \times 10^{4}$
s/(kJ kg^{-1} K^{-1})	$0.405\,427\,273 \times 10^{1}$	$0.485\,438\,792 \times 10^{1}$	$0.446\,971\,906 \times 10^{1}$
c_p/(kJ kg^{-1} K^{-1})	$0.138\,935\,717 \times 10^{2}$	$0.446\,579\,342 \times 10^{2}$	$0.634\,165\,359 \times 10^{1}$
w/(m s^{-1})	$0.502\,005\,554 \times 10^{3}$	$0.383\,444\,594 \times 10^{3}$	$0.760\,696\,041 \times 10^{3}$

[a] It is recommended to verify programmed functions using 8 byte real values for all three combinations of T and ρ given in this table.

8 Equations for Region 4

This section contains all details relevant for the use of the equations for region 4 of IAPWS-IF97 (saturation line). Information about the consistency of the basic equation for this region, the saturation-pressure equation, and the basic equations of regions 1 to 3 at the corresponding region boundaries is summarized in Section 10. The results of computing-time comparisons between IAPWS-IF97 and IFC-67 are given in Section 11. The estimates of uncertainty of the saturation pressure can be found in Section 12.

The equation for describing the saturation line is an implicit quadratic equation which can be directly solved with regard to both saturation pressure p_s and saturation temperature T_s. This equation reads

$$\beta^2\vartheta^2 + n_1\beta^2\vartheta + n_2\beta^2 + n_3\beta\vartheta^2 + n_4\beta\vartheta + n_5\beta + n_6\vartheta^2 + n_7\vartheta + n_8 = 0\,, \tag{29}$$

where
$$\beta = \left(p_\mathrm{s} / p^*\right)^{1/4} \tag{29a}$$

and
$$\vartheta = \frac{T_\mathrm{s}}{T^*} + \frac{n_9}{\left(T_\mathrm{s}/T^*\right) - n_{10}} \tag{29b}$$

with $p^* = 1$ MPa and $T^* = 1$ K; for the coefficients n_1 to n_{10} see Table 34.

8.1 The Saturation-Pressure Equation (Basic Equation)

The solution of Eq. (29) with regard to saturation pressure is as follows:

$$\frac{p_\mathrm{s}}{p^*} = \left[\frac{2C}{-B + \left(B^2 - 4AC\right)^{1/2}}\right]^4 , \tag{30}$$

where $p^* = 1$ MPa and

$$A = \vartheta^2 + n_1\vartheta + n_2$$
$$B = n_3\vartheta^2 + n_4\vartheta + n_5$$
$$C = n_6\vartheta^2 + n_7\vartheta + n_8$$

with ϑ according to Eq. (29b). The coefficients n_i of Eq. (30) are listed in Table 34.

Table 34. Numerical values of the coefficients of the dimensionless saturation equations, Eqs. (29) to (31)

i	n_i	i	n_i
1	$0.116\,705\,214\,527\,67 \times 10^{4}$	6	$0.149\,151\,086\,135\,30 \times 10^{2}$
2	$-0.724\,213\,167\,032\,06 \times 10^{6}$	7	$-0.482\,326\,573\,615\,91 \times 10^{4}$
3	$-0.170\,738\,469\,400\,92 \times 10^{2}$	8	$0.405\,113\,405\,420\,57 \times 10^{6}$
4	$0.120\,208\,247\,024\,70 \times 10^{5}$	9	$-0.238\,555\,575\,678\,49$
5	$-0.323\,255\,503\,223\,33 \times 10^{7}$	10	$0.650\,175\,348\,447\,98 \times 10^{3}$

Equations (29) to (31) reproduce exactly the p-T values at the triple point according to Eq. (9), at the normal boiling point [12] and at the critical point according to Eqs. (2) and (3).

Range of validity

Equation (30) is valid along the entire vapor-liquid saturation line from the triple-point temperature T_t to the critical temperature T_c and can be simply extrapolated to 273.15 K so that it covers the temperature range

$$273.15 \text{ K} \le T \le 647.096 \text{ K}.$$

Computer-program verification

To assist the user in computer-program verification of Eq. (30), Table 35 contains test values for three selected temperatures.

Table 35. Saturation pressures calculated from Eq. (30) for selected values of T [a]

T/K	p_s/MPa
300	$0.353\,658\,941 \times 10^{-2}$
500	$0.263\,889\,776 \times 10^{1}$
600	$0.123\,443\,146 \times 10^{2}$

[a] It is recommended to verify the programmed equation using 8 byte real values for all three values of T given in this table.

8.2 The Saturation-Temperature Equation (Backward Equation)

The saturation-temperature solution of Eq. (29) reads

$$\frac{T_\mathrm{s}}{T^*} = \frac{n_{10} + D - \left[\left(n_{10} + D \right)^2 - 4 \left(n_9 + n_{10} D \right) \right]^{1/2}}{2} \ , \qquad (31)$$

where $T^* = 1$ K and

$$D = \frac{2G}{-F - \left(F^2 - 4EG \right)^{1/2}}$$

with

$$E = \beta^2 + n_3 \beta + n_6$$

$$F = n_1 \beta^2 + n_4 \beta + n_7$$

$$G = n_2 \beta^2 + n_5 \beta + n_8$$

and β according to Eq. (29a). The coefficients n_i of Eq. (31) are listed in Table 34.

Range of validity

Equation (31) has the same range of validity as Eq. (30), which means that it covers the vapor-liquid saturation line according to the pressure range

$$611.213 \text{ Pa} \le p \le 22.064 \text{ MPa} \ .$$

The value of 611.213 Pa corresponds to the pressure when Eq. (31) is extrapolated to 273.15 K.

Consistency with the basic equation

Since the saturation-pressure equation, Eq. (30), and the saturation-temperature equation, Eq. (31), have been derived from the same implicit equation, Eq. (29), for describing the saturation line, both Eq. (30) and Eq. (31) are *completely* consistent with each other.

Computer-program verification

To assist the user in computer-program verification of Eq. (31), Table 36 contains test values for three selected pressures.

Table 36. Saturation temperatures calculated from Eq. (31) for selected values of p [a]

p/MPa	T_s/K
0.1	$0.372\,755\,919 \times 10^3$
1	$0.453\,035\,632 \times 10^3$
10	$0.584\,149\,488 \times 10^3$

[a] It is recommended to verify the programmed equation using 8 byte real values for all three values of p given in this table.

9 Basic Equation for Region 5

This section contains all details relevant for the use of the equations for region 5 of IAPWS-IF97. Information about the consistency at the boundary between regions 2 and 5 is summarized in Section 10. The results of computing-time comparisons between IAPWS-IF97 and IFC-67 are given in Section 11. The estimates of uncertainty of the most relevant properties can be found in Section 12.

The basic equation for this high-temperature region is a fundamental equation for the specific Gibbs free energy g. This equation is expressed in dimensionless form, $\gamma = g/(RT)$, and is separated into two parts, an ideal-gas part γ^{o} and a residual part γ^{r}, so that

$$\frac{g(p,T)}{RT} = \gamma(\pi,\tau) = \gamma^{\mathrm{o}}(\pi,\tau) + \gamma^{\mathrm{r}}(\pi,\tau) \ , \qquad (32)$$

where $\pi = p/p^*$ and $\tau = T^*/T$ with R given by Eq. (1).

The equation for the ideal-gas part γ^{o} of the dimensionless Gibbs free energy reads

$$\gamma^{\mathrm{o}} = \ln \pi + \sum_{i=1}^{6} n_i^{\mathrm{o}} \tau^{J_i^{\mathrm{o}}} \ , \qquad (33)$$

where $\pi = p/p^*$ and $\tau = T^*/T$ with $p^* = 1$ MPa and $T^* = 1000$ K. The coefficients n_1^{o} and n_2^{o} were adjusted in such a way that the values for the specific internal energy and specific entropy in the ideal-gas state relate to Eq. (8). Table 37 contains the coefficients n_i^{o} and exponents J_i^{o} of Eq. (33).

Table 37. Numerical values of the coefficients and exponents of the ideal-gas part γ^{o} of the dimensionless Gibbs free energy for region 5, Eq. (33)

i	J_i^{o}	n_i^{o}	i	J_i^{o}	n_i^{o}
1	0	$-0.131\,799\,836\,742\,01 \times 10^{2}$	4	-2	$0.369\,015\,349\,803\,33$
2	1	$0.685\,408\,416\,344\,34 \times 10^{1}$	5	-1	$-0.311\,613\,182\,139\,25 \times 10^{1}$
3	-3	$-0.248\,051\,489\,334\,66 \times 10^{-1}$	6	2	$-0.329\,616\,265\,389\,17$

The form of the residual part γ^{r} of the dimensionless Gibbs free energy is as follows:

$$\gamma^{\mathrm{r}} = \sum_{i=1}^{6} n_i \, \pi^{I_i} \tau^{J_i} \quad , \tag{34}$$

where $\pi = p/p^*$ and $\tau = T^*/T$ with $p^* = 1$ MPa and $T^* = 1000$ K. The coefficients n_i and exponents I_i and J_i of Eq. (34) are listed in Table 38.

All thermodynamic properties can be derived from Eq. (32) by using the appropriate combinations of the ideal-gas part γ^{o}, Eq. (33), and the residual part γ^{r}, Eq. (34), of the dimensionless Gibbs free energy and their derivatives. Relations between the relevant thermodynamic properties and γ^{o} and γ^{r} and their derivatives are summarized in Table 39. All required derivatives of the ideal-gas part and of the residual part of the dimensionless Gibbs free energy are explicitly given in Table 40 and Table 41, respectively.

Table 38. Numerical values of the coefficients and exponents of the residual part γ^{r} of the dimensionless Gibbs free energy for region 5, Eq. (34)

i	I_i	J_i	n_i
1	1	1	$0.157\,364\,048\,552\,59 \times 10^{-2}$
2	1	2	$0.901\,537\,616\,739\,44 \times 10^{-3}$
3	1	3	$-0.502\,700\,776\,776\,48 \times 10^{-2}$
4	2	3	$0.224\,400\,374\,094\,85 \times 10^{-5}$
5	2	9	$-0.411\,632\,754\,534\,71 \times 10^{-5}$
6	3	7	$0.379\,194\,548\,229\,55 \times 10^{-7}$

Table 39. Relations of thermodynamic properties to the ideal-gas part γ^{o} and the residual part γ^{r} of the dimensionless Gibbs free energy and their derivatives [a] when using Eq. (32)

Property	Relation
Specific volume $v = (\partial g/\partial p)_T$	$v(\pi,\tau)\dfrac{p}{RT} = \pi\left(\gamma^{\mathrm{o}}_{\pi} + \gamma^{\mathrm{r}}_{\pi}\right)$
Specific internal energy $u = g - T(\partial g/\partial T)_p - p(\partial g/\partial p)_T$	$\dfrac{u(\pi,\tau)}{RT} = \tau\left(\gamma^{\mathrm{o}}_{\tau} + \gamma^{\mathrm{r}}_{\tau}\right) - \pi\left(\gamma^{\mathrm{o}}_{\pi} + \gamma^{\mathrm{r}}_{\pi}\right)$
Specific entropy $s = -(\partial g/\partial T)_p$	$\dfrac{s(\pi,\tau)}{R} = \tau\left(\gamma^{\mathrm{o}}_{\tau} + \gamma^{\mathrm{r}}_{\tau}\right) - \left(\gamma^{\mathrm{o}} + \gamma^{\mathrm{r}}\right)$
Specific enthalpy $h = g - T(\partial g/\partial T)_p$	$\dfrac{h(\pi,\tau)}{RT} = \tau\left(\gamma^{\mathrm{o}}_{\tau} + \gamma^{\mathrm{r}}_{\tau}\right)$
Specific isobaric heat capacity $c_p = (\partial h/\partial T)_p$	$\dfrac{c_p(\pi,\tau)}{R} = -\tau^2\left(\gamma^{\mathrm{o}}_{\tau\tau} + \gamma^{\mathrm{r}}_{\tau\tau}\right)$
Specific isochoric heat capacity $c_v = (\partial u/\partial T)_v$	$\dfrac{c_v(\pi,\tau)}{R} = -\tau^2\left(\gamma^{\mathrm{o}}_{\tau\tau} + \gamma^{\mathrm{r}}_{\tau\tau}\right) - \dfrac{(1+\pi\gamma^{\mathrm{r}}_{\pi} - \tau\pi\gamma^{\mathrm{r}}_{\pi\tau})^2}{1-\pi^2\gamma^{\mathrm{r}}_{\pi\pi}}$
Speed of sound $w = v\left[-(\partial p/\partial v)_s\right]^{1/2}$	$\dfrac{w^2(\pi,\tau)}{RT} = \dfrac{1 + 2\pi\gamma^{\mathrm{r}}_{\pi} + \pi^2\gamma^{\mathrm{r}\,2}_{\pi}}{\left(1-\pi^2\gamma^{\mathrm{r}}_{\pi\pi}\right) + \dfrac{\left(1+\pi\gamma^{\mathrm{r}}_{\pi} - \tau\pi\gamma^{\mathrm{r}}_{\pi\tau}\right)^2}{\tau^2\left(\gamma^{\mathrm{o}}_{\tau\tau} + \gamma^{\mathrm{r}}_{\tau\tau}\right)}}$

[a] $\gamma^{\mathrm{r}}_{\pi} = \left[\dfrac{\partial\gamma^{\mathrm{r}}}{\partial\pi}\right]_{\tau}$, $\gamma^{\mathrm{r}}_{\pi\pi} = \left[\dfrac{\partial^2\gamma^{\mathrm{r}}}{\partial\pi^2}\right]_{\tau}$, $\gamma^{\mathrm{r}}_{\tau} = \left[\dfrac{\partial\gamma^{\mathrm{r}}}{\partial\tau}\right]_{\pi}$, $\gamma^{\mathrm{r}}_{\tau\tau} = \left[\dfrac{\partial^2\gamma^{\mathrm{r}}}{\partial\tau^2}\right]_{\pi}$, $\gamma^{\mathrm{r}}_{\pi\tau} = \left[\dfrac{\partial^2\gamma^{\mathrm{r}}}{\partial\pi\partial\tau}\right]$,

$\gamma^{\mathrm{o}}_{\tau} = \left[\dfrac{\partial\gamma^{\mathrm{o}}}{\partial\tau}\right]_{\pi}$, $\gamma^{\mathrm{o}}_{\tau\tau} = \left[\dfrac{\partial^2\gamma^{\mathrm{o}}}{\partial\tau^2}\right]_{\pi}$

Table 40. The ideal-gas part γ^{o} of the dimensionless Gibbs free energy and its derivatives [a] according to Eq. (33)

$$\gamma^{\mathrm{o}} = \ln\pi + \sum_{i=1}^{6} n_i^{\mathrm{o}} \tau^{J_i^{\mathrm{o}}}$$

$$\gamma_{\pi}^{\mathrm{o}} = 1/\pi + 0$$

$$\gamma_{\pi\pi}^{\mathrm{o}} = -1/\pi^2 + 0$$

$$\gamma_{\tau}^{\mathrm{o}} = 0 + \sum_{i=1}^{6} n_i^{\mathrm{o}} J_i^{\mathrm{o}} \tau^{J_i^{\mathrm{o}}-1}$$

$$\gamma_{\tau\tau}^{\mathrm{o}} = 0 + \sum_{i=1}^{6} n_i^{\mathrm{o}} J_i^{\mathrm{o}} \left(J_i^{\mathrm{o}}-1\right) \tau^{J_i^{\mathrm{o}}-2}$$

$$\gamma_{\pi\tau}^{\mathrm{o}} = 0 + 0$$

[a] $\gamma_{\pi}^{\mathrm{o}} = \left[\frac{\partial \gamma^{\mathrm{o}}}{\partial \pi}\right]_{\tau}$, $\gamma_{\pi\pi}^{\mathrm{o}} = \left[\frac{\partial^2 \gamma^{\mathrm{o}}}{\partial \pi^2}\right]_{\tau}$, $\gamma_{\tau}^{\mathrm{o}} = \left[\frac{\partial \gamma^{\mathrm{o}}}{\partial \tau}\right]_{\pi}$, $\gamma_{\tau\tau}^{\mathrm{o}} = \left[\frac{\partial^2 \gamma^{\mathrm{o}}}{\partial \tau^2}\right]_{\pi}$, $\gamma_{\pi\tau}^{\mathrm{o}} = \left[\frac{\partial^2 \gamma^{\mathrm{o}}}{\partial \pi \partial \tau}\right]$

Table 41. The residual part γ^{r} of the dimensionless Gibbs free energy and its derivatives [a] according to Eq. (34)

$$\gamma^{\mathrm{r}} = \sum_{i=1}^{6} n_i \, \pi^{I_i} \, \tau^{J_i}$$

$$\gamma_{\pi}^{\mathrm{r}} = \sum_{i=1}^{6} n_i \, I_i \, \pi^{I_i-1} \, \tau^{J_i} \qquad \gamma_{\pi\pi}^{\mathrm{r}} = \sum_{i=1}^{6} n_i \, I_i \left(I_i - 1\right) \pi^{I_i-2} \, \tau^{J_i}$$

$$\gamma_{\tau}^{\mathrm{r}} = \sum_{i=1}^{6} n_i \, \pi^{I_i} J_i \, \tau^{J_i-1} \qquad \gamma_{\tau\tau}^{\mathrm{r}} = \sum_{i=1}^{6} n_i \, \pi^{I_i} J_i \left(J_i - 1\right) \tau^{J_i-2}$$

$$\gamma_{\pi\tau}^{\mathrm{r}} = \sum_{i=1}^{6} n_i \, I_i \, \pi^{I_i-1} J_i \, \tau^{J_i-1}$$

[a] $\gamma_{\pi}^{\mathrm{r}} = \left[\frac{\partial \gamma^{\mathrm{r}}}{\partial \pi}\right]_{\tau}$, $\gamma_{\pi\pi}^{\mathrm{r}} = \left[\frac{\partial^2 \gamma^{\mathrm{r}}}{\partial \pi^2}\right]_{\tau}$, $\gamma_{\tau}^{\mathrm{r}} = \left[\frac{\partial \gamma^{\mathrm{r}}}{\partial \tau}\right]_{\pi}$, $\gamma_{\tau\tau}^{\mathrm{r}} = \left[\frac{\partial^2 \gamma^{\mathrm{r}}}{\partial \tau^2}\right]_{\pi}$, $\gamma_{\pi\tau}^{\mathrm{r}} = \left[\frac{\partial^2 \gamma^{\mathrm{r}}}{\partial \pi \partial \tau}\right]$

Range of validity

Equation (32) covers region 5 of IAPWS-IF97 defined by the following temperature and pressure range:

$$1073.15\ \mathrm{K} \le T \le 2273.15\ \mathrm{K} \qquad 0 < p \le 50\ \mathrm{MPa}\,.$$

Equation (32) is only valid for pure undissociated water; any dissociation will have to be taken into account separately.

Computer-program verification

To assist the user in computer-program verification of Eq. (32), Table 42 contains test values of the most relevant properties.

Table 42. Thermodynamic property values calculated from Eq. (32) for selected values of T and p [a]

	T = 1500 K, p = 0.5 MPa	T = 1500 K, p = 30 MPa	T = 2000 K, p = 30 MPa
$v/(\mathrm{m^3\ kg^{-1}})$	$0.138\,455\,090 \times 10^{1}$	$0.230\,761\,299 \times 10^{-1}$	$0.311\,385\,219 \times 10^{-1}$
$h/(\mathrm{kJ\ kg^{-1}})$	$0.521\,976\,855 \times 10^{4}$	$0.516\,723\,514 \times 10^{4}$	$0.657\,122\,604 \times 10^{4}$
$u/(\mathrm{kJ\ kg^{-1}})$	$0.452\,749\,310 \times 10^{4}$	$0.447\,495\,124 \times 10^{4}$	$0.563\,707\,038 \times 10^{4}$
$s/(\mathrm{kJ\ kg^{-1}\ K^{-1}})$	$0.965\,408\,875 \times 10^{1}$	$0.772\,970\,133 \times 10^{1}$	$0.853\,640\,523 \times 10^{1}$
$c_p/(\mathrm{kJ\ kg^{-1}\ K^{-1}})$	$0.261\,609\,445 \times 10^{1}$	$0.272\,724\,317 \times 10^{1}$	$0.288\,569\,882 \times 10^{1}$
$w/(\mathrm{m\ s^{-1}})$	$0.917\,068\,690 \times 10^{3}$	$0.928\,548\,002 \times 10^{3}$	$0.106\,736\,948 \times 10^{4}$

[a] It is recommended to verify programmed functions using 8 byte real values for all three combinations of T and p given in this table.

10 Consistency at Region Boundaries

For any calculation of thermodynamic properties of water and steam across the region boundaries, the equations of IAPWS-IF97 have to be sufficiently consistent along the corresponding boundary. For the properties considered in this respect, this section presents the achieved consistencies in comparison to the permitted inconsistencies according to the so-called Prague values [13].

10.1 Consistency at Boundaries between Single-Phase Regions

For the boundaries between single-phase regions, the consistency investigations were performed for the following basic equations and region boundaries; see Fig. 1:

- Equations (7) and (28) along the 623.15 K isotherm for pressures from 16.53 MPa (p_s from Eq. (30) for 623.15 K) to 100 MPa corresponding to the boundary between regions 1 and 3.

- Equations (15) and (28) with respect to the boundary between regions 2 and 3 defined by the B23-equation, Eq. (5), for temperatures between 623.15 K and 863.15 K.

- Equations (15) and (32) with respect to the 1073.15 K isotherm for $p \le 50$ MPa corresponding to the boundary between regions 2 and 5.

The results of the consistency investigations for these three region boundaries are summarized in Table 43. In addition to the permitted inconsistencies corresponding to the Prague values [13], the actual inconsistencies characterized by their maximum and root-mean-square values, $|\Delta x|_{\max}$ and Δx_{RMS}, along the three boundaries are given for $x = v$, h, c_p, s, g, and w. It can be seen that the inconsistencies between the basic equations along the corresponding region boundaries are extremely small.

Table 43. Inconsistencies between basic equations for single-phase regions at the joint region boundary

Inconsistency Δx	Prague value	Regions 1/3 Eqs. (7)/(28)		Regions 2/3 Eqs. (15)/(28)		Regions 2/5 Eqs. (15)/(32)	
		$\|\Delta x\|_{\max}$	Δx_{RMS} [a]	$\|\Delta x\|_{\max}$	Δx_{RMS} [a]	$\|\Delta x\|_{\max}$	Δx_{RMS} [a]
$\|\Delta v\|$ / %	0.05	0.004	0.002	0.018	0.007	0.012	0.007
$\|\Delta h\|$ / (kJ kg^{-1})	0.2	0.031	0.014	0.134	0.073	0.096	0.070
$\|\Delta c_p\|$ / %	1	0.195	0.058	0.353	0.169	0.074	0.049
$\|\Delta s\|$ / (J kg^{-1} K^{-1})	0.2	0.042	0.022	0.177	0.094	0.142	0.084
$\|\Delta g\|$ / (kJ kg^{-1})	0.2	0.005	0.005	0.005	0.003	0.087	0.072
$\|\Delta w\|$ / %	1 [b]	0.299	0.087	0.403	0.073	0.046	0.028

[a] The Δx_{RMS} values (see Nomenclature) were calculated from about 10 000 points evenly distributed along the corresponding boundary.

[b] The permitted inconsistency value for w is not included in the Prague values [13].

10.2 Consistency at the Saturation Line

The consistency investigations along the vapor-liquid saturation line were performed for the properties p_{s}, T_{s}, and g. The calculations concern the following basic equations and ranges of the saturation line, see Fig. 1; the way of calculating the inconsistencies Δp_{s}, ΔT_{s}, and Δg is also given:

- Equations (7), (15) and (30) on the saturation line for temperatures from $T_{\mathrm{t}} = 273.15$ K to 623.15 K.

$$
\begin{aligned}
\Delta p_\mathrm{s} &= p_{\mathrm{s,\,Eq.(7),\,Eq.(15)}} - p_{\mathrm{s,\,Eq.(30)}} && \text{(35a)}\\
\Delta T_\mathrm{s} &= T_{\mathrm{s,\,Eq.(7),\,Eq.(15)}} - T_{\mathrm{s,\,Eq.(31)}} && \text{(35b)}\\
\Delta g &= g_{\mathrm{Eq.(7)}} - g_{\mathrm{Eq.(15)}} && \text{(35c)}
\end{aligned}
$$

The calculation of p_s and of T_s from Eqs. (7) and (15) is made via the Maxwell criterion (phase-equilibrium condition) for given values of T or p. The g values are determined for given T values and corresponding p_s values from Eq. (30).

- Equations (28) and (30) on the saturation line for temperatures from 623.15 K to T_c = 647.096 K.

$$
\begin{aligned}
\Delta p_\mathrm{s} &= p_{\mathrm{s,\,Eq.(28)}} - p_{\mathrm{s,\,Eq.(30)}} && \text{(36a)}\\
\Delta T_\mathrm{s} &= T_{\mathrm{s,\,Eq.(28)}} - T_{\mathrm{s,\,Eq.(31)}} && \text{(36b)}\\
\Delta g &= g'_{\mathrm{Eq.(28),\,Eq.(30)}} - g''_{\mathrm{Eq.(28),\,Eq.(30)}} && \text{(36c)}
\end{aligned}
$$

The calculation of p_s and T_s from Eq. (28) is made via the Maxwell criterion for given temperatures or pressures, respectively. The inconsistency Δg corresponds to the difference $g'(\rho',T) - g''(\rho'',T)$ which is calculated from Eq. (28) after ρ' and ρ'' are determined from Eq. (28) by iteration for given T values and corresponding p_s values from Eq. (30).

- Equations (7), (15) and (28) on the saturation line at 623.15 K. This is the only point on the saturation line where the validity ranges of the fundamental equations of regions 1 to 3 meet each other.

$$
\begin{aligned}
\Delta p_\mathrm{s} &= p_{\mathrm{s,\,Eq.(7),\,Eq.(15)}} - p_{\mathrm{s,\,Eq.(28)}} && \text{(37a)}\\
\Delta T_\mathrm{s} &= T_{\mathrm{s,\,Eq.(7),\,Eq.(15)}} - T_{\mathrm{s,\,Eq.(28)}} && \text{(37b)}\\
\Delta g &= g_{\mathrm{Eq.(7),\,Eq.(15)}} - g_{\mathrm{Eq.(28)}} && \text{(37c)}
\end{aligned}
$$

All three properties p_s and T_s and g are calculated via the Maxwell criterion from the corresponding equations.

The results of these consistency investigations along the saturation line are summarized in Table 44. In addition to the permitted inconsistencies corresponding to the Prague values [13], the actual inconsistencies characterized by their maximum and root-mean-square values, $|\Delta x|_\mathrm{max}$ and Δx_RMS, for the two sections of the saturation line are given for $x = p_\mathrm{s}$, T_s and g. It can be seen that the inconsistencies between the basic equations for the corresponding single-phase region and the saturation-pressure equation are extremely small. This statement also holds for the fundamental equations, Eqs. (7), (15), and (28), among one another and not only in relation to the saturation-pressure equation, Eq. (30), see the last column in Table 44.

Table 44. Inconsistencies between the basic equations valid at the saturation line

Inconsistency Δx	Prague value	$T_t \le T \le 623.15$ K Eqs. (7),(15)/(30)		623.15 K $\le T \le T_c$ Eqs. (28)/(30)		$T = 623.15$ K Eqs. (7),(15)/(28)
		$\lvert\Delta x\rvert_{max}$	Δx_{RMS} [a]	$\lvert\Delta x\rvert_{max}$	Δx_{RMS} [a]	
$\lvert\Delta p_s\rvert$ / %	0.05	0.0069	0.0033	0.0026	0.0015	0.0041
$\lvert\Delta T_s\rvert$ / %	0.02	0.0006	0.0003	0.0003	0.0002	0.0006
$\lvert\Delta g\rvert$ / (kJ kg^{-1})	0.2	0.012	0.006	0.002	0.001	0.005

[a] The Δx_{RMS} values (see Nomenclature) were calculated from about 3000 points evenly distributed along the two sections of the saturation line.

11 Computing Time of IAPWS-IF97 in Relation to IFC-67

A very important requirement for IAPWS-IF97 was that its computing speed in relation to IFC-67 should be significantly faster. The computation-speed investigations of IAPWS-IF97 in comparison with IFC-67 are based on a special procedure agreed to by IAPWS.

The computing times were measured with a benchmark program developed by IAPWS; this program calculates the corresponding functions at a large number of state points well distributed proportionately over each region. The test configuration agreed on was a PC Intel 486 DX 33 processor and the MS Fortran 5.1 compiler. The relevant functions of IAPWS-IF97 were programmed with regard to short computing times. The calculations with IFC-67 were carried out with the ASME program package [14] speeded up by excluding all parts which were not needed for these special benchmark tests.

The measured computing times were used to calculate computing-time ratios IFC-67/IAPWS-IF97, called CTR values in the following. These CTR values, determined in a different way for regions 1, 2, and 4 (see Section 11.1) and for regions 3 and 5 (see Section 11.2), are the characteristic quantities for the judgment of how much faster the calculations with IAPWS-IF97 are in comparison with IFC-67. Metastable states are not included in these investigations.

11.1 Computing-Time Investigations for Regions 1, 2, and 4

The computing-time investigations for regions 1, 2, and 4, which are particularly relevant to computing time, were performed for the functions listed in Table 45. Each function is associated with a frequency-of-use value. Both the selection of the functions and the values for the corresponding frequency of use are based on a worldwide survey made among the power plant companies and related industries.

For the computing-time comparison between IAPWS-IF97 and IFC-67 for regions 1, 2, and 4, the *total* CTR value of these three regions together was the decisive criterion, where the frequencies of use have to be taken into account. The total CTR value was calculated as follows: As has been described before, the computing times for each function were determined for IFC-67 and for IAPWS-IF97. Then, these values were weighted by the corresponding frequencies of use and added up for the 16 functions of the three regions. The total CTR value is obtained from the sum of the weighted computing times for IFC-67 divided by the corresponding value for IAPWS-IF97. The total CTR value for regions 1, 2, and 4 amounts to

$$\mathrm{CTR}_{\text{regions }1,2,4} = 5.1\ . \tag{38}$$

This means that for regions 1, 2, and 4 together the property calculations with IAPWS-IF97 are more than five times faster than with IFC-67.

Table 45. Results of the computing-time investigations of IAPWS-IF97 in relation to IFC-67 for regions 1, 2, and 4[a]

Region[b]	Function	Frequency of use %	Computing-time ratio IFC-67 / IF97
1	$v(p,T)$	2.9	2.7
	$h(p,T)$	9.7	2.9
	$T(p,h)$	3.5	24.8
	$h(p,s)$	1.2	10.0
		Σ region 1:	5.6[c]
2	$v(p,T)$	6.1	2.1
	$h(p,T)$	12.1	2.9
	$s(p,T)$	1.4	1.4
	$T(p,h)$	8.5	12.4
	$v(p,h)$	3.1	6.4
	$s(p,h)$	1.7	4.2
	$T(p,s)$	1.7	8.1
	$h(p,s)$	4.9	5.6
		Σ region 2:	5.0[c]
4	$p_s(T)$	8.0	1.7
	$T_s(p)$	30.7	5.6
	$h'(p)$	2.25	4.4
	$h''(p)$	2.25	4.2
		Σ region 4:	4.9[c]
		Σ regions 1, 2 and 4:	**5.1**[c]

[a] Based on the agreed PC Intel 486 DX 33 with MS Fortran 5.1 compiler.
[b] For the definition of the regions see Fig. 1.
[c] This CTR value is based on the computing times for the single functions weighted by the frequency-of-use values; see text.

Table 45 also contains total CTR values separately for each of regions 1, 2, and 4. In addition, CTR values for each single function are given. When using IAPWS-IF97 the functions depending on p,h and p,s for regions 1 and 2 and on p for region 4 were calculated from the backward equations alone (functions explicit in T) or from the basic equations in combination with the corresponding backward equation.

If a faster processor than specified above is used for the described benchmark tests, similar CTR values are obtained. A corresponding statement is also valid for other compilers than the specified one.

11.2 Computing-Time Investigations for Region 3

For regions 3 and 5 the CTR values only relate to single functions and are given by the quotient of the computing time needed for IFC-67 calculation and the computing time when using IAPWS-IF97; there are no frequency-of-use values for functions relevant to these two regions.

For region 3 of IAPWS-IF97, corresponding to regions 3 and 4 of IFC-67, the computing-time investigations relate to the functions $p(v,T)$, $h(v,T)$, $c_p(v,T)$, and $s(v,T)$ where 10 % of the test points are in region 4 of IFC-67.

Table 46 lists the CTR values obtained for the relevant functions of region 3. Roughly speaking, IAPWS-IF97 is more than three times faster than IFC-67 for this region.

Table 46. Results of the computing-time investigations of IAPWS-IF97 in relation to IFC-67 for region 3[a]

Function	Computing time ratio IFC-67/IF97
$p(v,T)$	3.8
$h(v,T)$	4.3
$c_p(v,T)$	2.9
$s(v,T)$	3.2

[a] Based on the agreed PC Intel 486 DX 33 with MS Fortran 5.1 compiler.

12 Estimates of Uncertainties

Estimates have been made of the uncertainty of the specific volume, specific isobaric heat capacity, speed of sound, and saturation pressure when calculated from the corresponding equations of IAPWS-IF97. These estimates were derived from the uncertainties of IAPWS-95 [3], from which the input values for fitting the IAPWS-IF97 equations were calculated, and in addition by taking into account the deviations between the corresponding values calculated from IAPWS-IF97 and IAPWS-95. Since there is no reasonable basis for estimating the uncertainty of specific enthalpy (because specific enthalpy is dependent on the selection of the zero point, only enthalpy differences of different size are of interest), no uncertainty is given for this property. However, the uncertainty of isobaric enthalpy differences is smaller than the uncertainty in the isobaric heat capacity.

For the single-phase region, tolerances are indicated in Figs. 3 to 5 which give the estimated uncertainties in various areas. As used here "tolerance" means the range of possible values as judged by IAPWS, and no statistical significance can be attached to it. With regard to the uncertainty for the speed of sound and the specific isobaric heat capacity, see Figs. 4 and 5, it should be noted that the uncertainties for these properties increase drastically when approaching the critical point. The statement "no definitive uncertainty estimates possible" for temperatures above 1273 K is based on the fact that this range is beyond the range of validity of IAPWS-95 and the corresponding input values for IAPWS-IF97 were extrapolated from IAPWS-95. From various tests of IAPWS-95 [3] it is expected that these extrapolations yield reasonable values.

For the saturation pressure, the estimate of uncertainty is shown in Fig. 6.

Estimated uncertainties in enthalpy, in enthalpy differences in the single-phase region, and in the enthalpy of vaporization are given in IAPWS Advisory Note No. 1 [15].

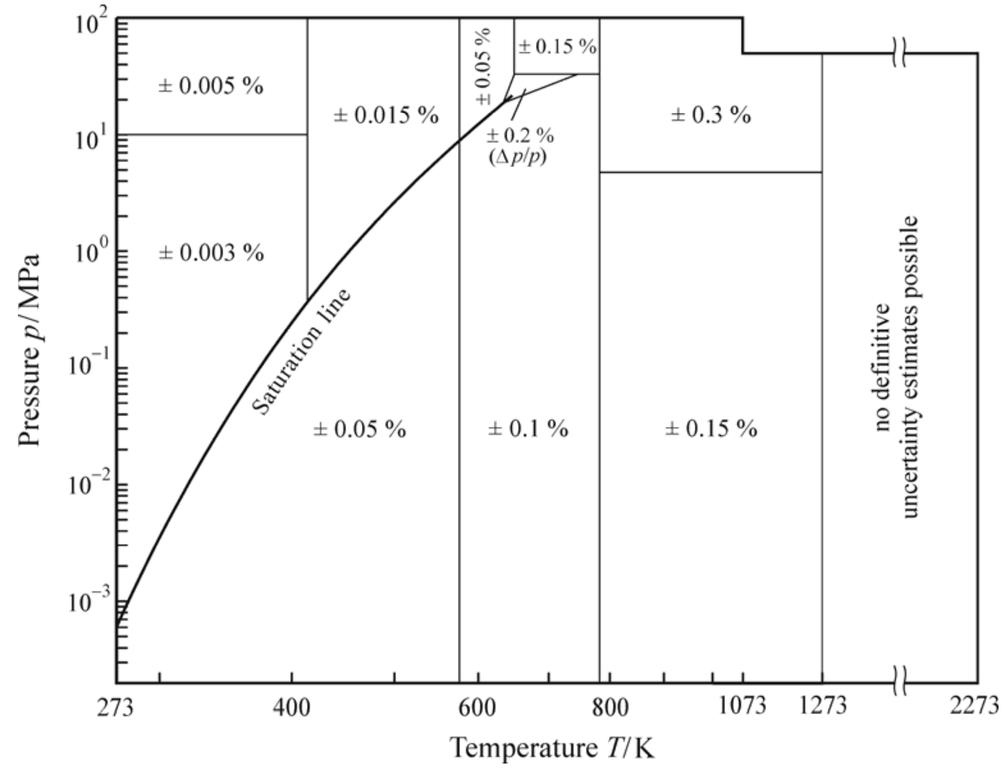

Fig. 3. Uncertainties in specific volume, $\Delta v/v$, estimated for the corresponding equations of IAPWS-IF97. In the enlarged critical region (triangle), the uncertainty is given as percentage uncertainty in pressure, $\Delta p/p$. This region is bordered by the two isochores $0.0019\ \mathrm{m^3\,kg^{-1}}$ and $0.0069\ \mathrm{m^3\,kg^{-1}}$ and by the 30 MPa isobar. The positions of the lines separating the uncertainty regions are approximate.

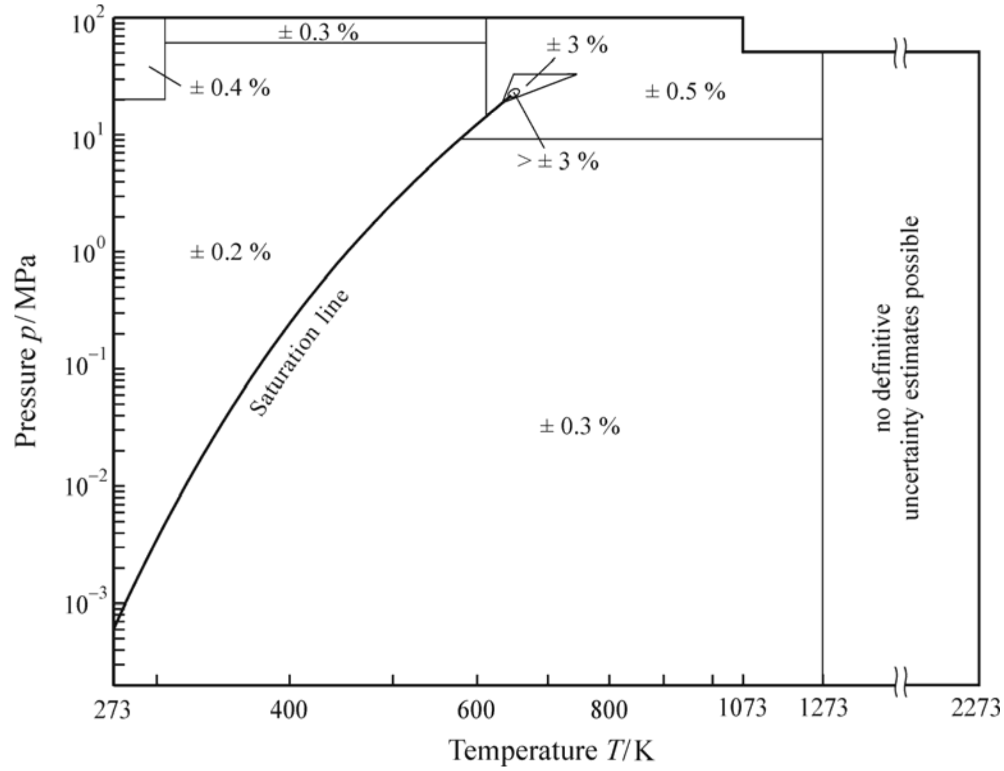

Fig. 4. Uncertainties in specific isobaric heat capacity, $\Delta c_p/c_p$, estimated for the corresponding equations of IAPWS-IF97. For the definition of the triangle around the critical point, see Fig. 3. The positions of the lines separating the uncertainty regions are approximate.

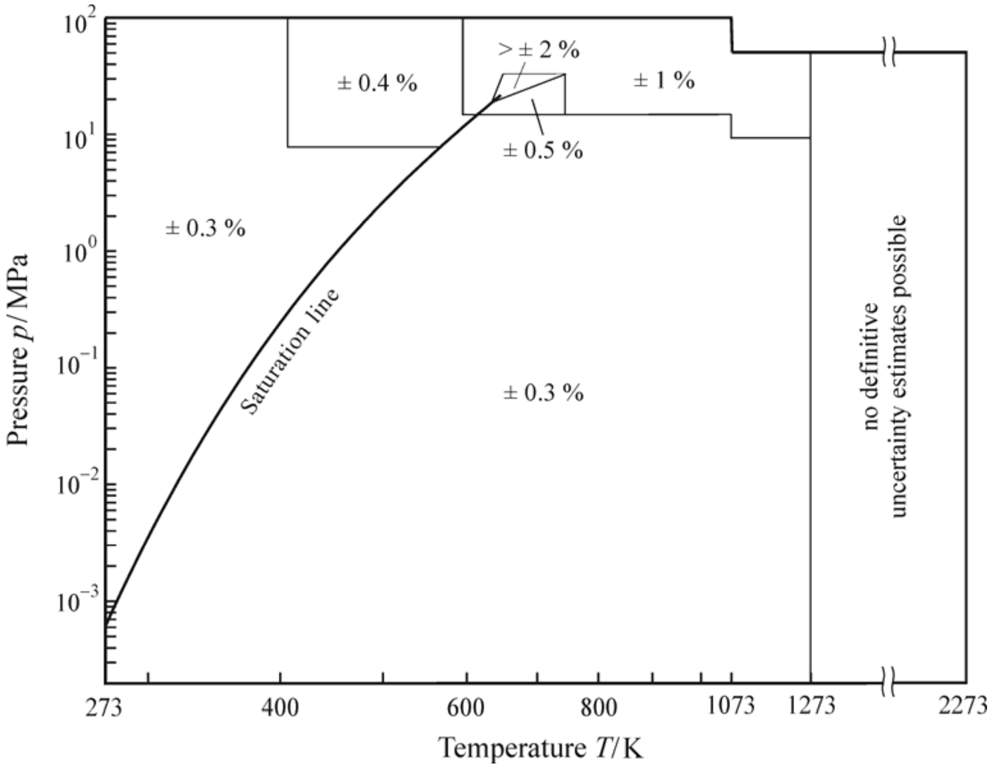

Fig. 5. Uncertainties in speed of sound, $\Delta w/w$, estimated for the corresponding equations of IAPWS-IF97. For the definition of the triangle around the critical point, see Fig. 3. The positions of the lines separating the uncertainty regions are approximate.

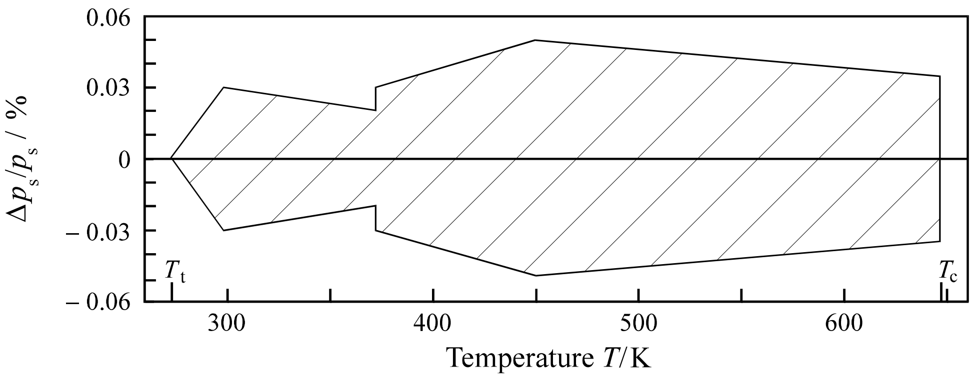

Fig. 6. Uncertainties in saturation pressure, $\Delta p_S/p_S$, estimated for the saturation-pressure equation, Eq. (30).

13 References

[1] International Formulation Committee of the 6th International Conference on the Properties of Steam, *The 1967 IFC Formulation for Industrial Use*, Verein Deutscher Ingenieure, Düsseldorf, 1967.

[2] Wagner, W., Cooper, J. R., Dittmann, A., Kijima, J., Kretzschmar, H.-J., Kruse, A., Mareš, R., Oguchi, K., Sato, H., Stöcker, I., Šifner, O., Takaishi, Y., Tanishita, I., Trübenbach, J., and Willkommen, Th., The IAPWS Industrial Formulation 1997 for the Thermodynamic Properties of Water and Steam, *J. Eng. Gas Turbines & Power* **122**, 150-182 (2000).

[2a] Wagner, W., Dauber, F., Kretzschmar, H.-J., Mareš, R., Miyagawa, K., Parry, W. T., and Span, R., The New Basic Equation for the Extended Region 5 of the Industrial Formulation IAPWS-IF97 for Water and Steam. To be submitted to *J. Eng. Gas Turbines & Power*.

[2b] IAPWS Advisory Note No. 2: *Roles of Various IAPWS Documents Concerning the Thermodynamic Properties of Ordinary Water Substance* (2009). Available from http://www.iapws.org

[3] IAPWS, *Revised Release on the IAPWS Formulation 1995 for the Thermodynamic Properties of Ordinary Water Substance for General and Scientific Use* (2009). Available from http://www.iapws.org

[4] Cohen, E. R. and Taylor, B. N., *The 1986 Adjustment of the Fundamental Physical Constants*, CODATA Bulletin No. 63, Committee on Data for Science and Technology, Int. Council of Scientific Unions, Pergamon Press, Oxford, 1986.

[5] Audi, G. and Wapstra, A. H., The 1993 atomic mass evaluation, (I) Atomic mass table, *Nuclear Physics A* **565**, 1-65 (1993).

[6] IUPAC Commission on the Atomic Weights and Isotopic Abundances, Subcommittee for Isotopic Abundance Measurements, Isotopic compositions of the elements 1989, *Pure Appl. Chem.* **63**, 991-1002 (1991).

[7] IAPWS, *Release on the Values of Temperature, Pressure and Density of Ordinary and Heavy Water Substances at Their Respective Critical Points* (1992). Available from http://www.iapws.org

[8] Preston-Thomas, H., The International Temperature Scale of 1990 (ITS-90), *Metrologia* **27**, 3-10 (1990).

[9] Guildner, L. A., Johnson, D. P., and Jones, F. E., Vapor Pressure of Water at Its Triple Point, *J. Res. Natl. Bur. Stand.* **80A**, 505-521 (1976).

[10] IAPWS, *Revised Release on the Pressure along the Melting and Sublimation Curves of Ordinary Water Substance* (2008). Available from http://www.iapws.org

[11] Wagner, W. and Pruß, A., The IAPWS Formulation 1995 for the Thermodynamic Properties of Ordinary Water Substance for General and Scientific Use, *J. Phys. Chem. Ref. Data* **31**, 387-535 (2002).

[12] IAPWS, *Revised Supplementary Release on Saturation Properties of Ordinary Water Substance* (1992). Available from http://www.iapws.org

[13] Minutes of the meetings of the International Formulation Committee of ICPS in Prague, 1965.

[14] McClintock, R. B. and Silvestri, G. J., *Formulations and iterative procedures for the calculation of properties of steam,* The American Society of Mechanical Engineers, New York, 1968.

[15] IAPWS Advisory Note No. 1: *Uncertainties in Enthalpy for the IAPWS Formulation 1995 for the Thermodynamic Properties of Ordinary Water Substance for General and Scientific Use (IAPWS-95) and the IAPWS Industrial Formulation 1997 for the Thermodynamic Properties of Water and Steam (IAPWS-IF97)* (2003). Available from http://www.iapws.org